DOI:10.14753/SE.2012.1628

Imaging and aberrometric analyses of diseases affecting biomechanical properties of the cornea
Modern disgnostic methods of keratoconus

Ph.D. thesis

Dr. Miháltz Kata

Semmelweis University

Clinical Medicine, Ph.D. School

Supervisor: Dr. Nagy Zoltán Zsolt DSC

Reviewers: Dr. Kerényi Ágnes Ph.D.
Dr. Farkas Ágnes Ph.D.

Chairman of comprehensive exam: Dr. Matolcsy András D.Sc.
Members of comprehensive exam: Dr. Füst Ágnes Ph.D.
Dr. Erdei Gábor Ph.D.

Budapest 2011

DOI:10.14753/SE.2012.1628

Contents

DOI:10.14753/SE.2012.1628

DOI:10.14753/SE.2012.1628

Abbreviations

ACD: anterior chamber depth

AIC: Akaike information criterion

ANOVA: analysis of variance

ASCRS: American Society of Cataract and Refractive Surgery

AUROC: area under the receiver operating characteristic curve

BCVA: best corrected visual acuity

BFS: best-fit sphere

BFTE: best fit toric ellipsoid reference body

CCT: central corneal thickness

CFA: confirmatory factor analysis

CL: contact lens

CRF: corneal resistance factor

CH: corneal hysteresis

CXL: corneal crosslinking

D: diopter

DLK: diffuse lamellar keratitis

GEE: generalized estimating equation

HORMS: higher-order root mean square

ICRS: intrastromal corneal ring segments

IOL: intraocular lens

K: keratometry

KISA: central keratometry (K) inferior (I) minus superior (S) average (A) keratometry

LASIK: laser-assisted in situ keratomileusis

LKP: lamellar keratoplasty

LOS: line of sight

OPD: optical path difference

ORA: ocular response analyzer

OSA: optical society of America

pIOL: phakic intraocular lens

PKP: penetrating keratoplasty

PMD: pellucid marginal degeneration

PRK: photorefractive keratectomy

QICC: quasi-likelihood under independence model criterion

RSB: residual stromal bed

RMS: root mean square

ROC: receiver operating characteristic

ROS: reactive oxygen species

SA: spherical aberration

SCE: Stiles-Crawford effect

SD: standard deviation

TCT: thinnest corneal thickness

TMS: topographic modeling system

UCVA: uncorrected visual acuity

US: ultrasound

DOI:10.14753/SE.2012.1628

1. Introduction

The cornea, a transparent tissue that covers the front of the eye, performs approximately 2/3 of the optical refraction and focuses light towards the lens and the retina. Thus, even slight variations in the shape of the cornea can significantly diminish visual performance. It is reported though, that localized loss of corneal thickness, and likely also degradation of corneal mechanical properties, cause gradual tissue protrusion, which results in a more conical appearance of the cornea that imposes blurred vision. Surgical interventions and diseases of corneal tissue have been found to result in substantial changes in corneal tissue structure, which can then also alter the biomechanical properties of the cornea. The surgical procedures used to perform corneal refractive surgery result in changes in the corneal tissue structure, which affect the corneal thickness (CCT) and curvature of the cornea. Corneal refractive surgery and corneal diseases thus can alter corneal biomechanics. Keratoconus is the most frequently occurring disease of the cornea caused by a non-inflammatory deterioration of the corneal structure (1).

Keratoconus, which was first described in detail in 1854, derives from the Greek words Kerato (cornea) and Konos (cone) (2). Keratoconus is the most common primary ectasia. It is a bilateral and asymmetric corneal degeneration characterized by localized corneal thinning which leads to protrusion of the thinned cornea (3,4). Corneal thinning normally occurs in the inferior-temporal as well as the central cornea, although superior localizations have also been described. The disease induces myopia, irregular astigmatism and has well defined slit lamp findings (5,6). It has well-described clinical signs, but early forms of the disease may go undetected unless the anterior corneal topography is studied. The diagnosis of more advanced keratoconus is not complicated, because of the typical biomicroscopic and topographic findings, but the detection of subclinical or forme fruste cases may impose difficulty. Early disease is now best detected with videokeratoscopy or elevation based topography (7,8). It is particularly important to detect the disease among refractive surgery candidates, as keratorefractive procedures may worsen their condition (9). Corneal protrusion causes high myopia and irregular astigmatism, affecting visual quality.

DOI:10.14753/SE.2012.1628

1. 1. Epidemiology

The incidence and prevalence of keratoconus in the general population has been estimated to be between 5 and 23, and 5.4 per 10,000, respectively. Differences on the rates reported are attributed to different definitions and diagnostic criteria employed between studies. However, it would not be surprising to expect an increase in the incidence and prevalence rates of this disease over the next few years with the current wide spread use of corneal topography leading to improved diagnosis(10). Keratoconus affects both genders, although it is unclear whether significant differences between males and females exist (11).

Keratoconus, classically, has its onset at puberty and is progressive until the third to fourth decade of life, when it usually arrests. It is most commonly an isolated condition, despite multiple singular reports of coexistence with other disorders. Commonly recognized associations include Down syndrome, Leber's congenital amaurosis, and connective tissue disorders. For example, patients with advanced keratoconus have been reported to have a high incidence of mitral valve prolapse. Atopy, eye rubbing, and hard contact lenses have also been reported to be highly associated with this disorder (3, 12).

1. 2. Clinical Features

The ocular symptoms and signs of keratoconus vary depending on disease severity. At incipient stages, also referred to as subclinical or frustre forms, keratoconus does not normally produce any symptoms and thus can go unnoticed by the patient and practitioner unless specific tests (i.e., corneal topography) are undertaken for diagnosis (2,3). Disease progression is manifested by a significant loss of visual acuity which cannot be compensated for with spectacles. Therefore, eye care practitioners should be suspicious about the presence of keratoconus when a visual acuity of 1,0 is difficult to achieve with increasing against-the-rule astigmatism. Near visual acuity is generally found to be better than expected from the refraction, distance visual acuity and age of the patient (13,14). The appearance of "scissor" shadows while performing retinoscopy suggests the development of irregular astigmatism. Through retinoscopy it is possible to estimate the location of the cone's apex and its diameter, and the adjustable spectacle corrected visual acuity achievable. The Charleux oil drop that is observed by backlighting the mydriatric pupil also poses a warning sign (2,3).

DOI:10.14753/SE.2012.1628

In moderate and advance cases of keratoconus, a hemosiderin arc or circle line, commonly known as Fleischer's ring (Figure 1), is frequently seen around the cone base. This line has been suggested to be an accumulation of iron deposits from the tear film onto the cornea as a result of severe corneal curvature changes induced by the disease and/or due to modification of the normal epithelial slide process (15,16).

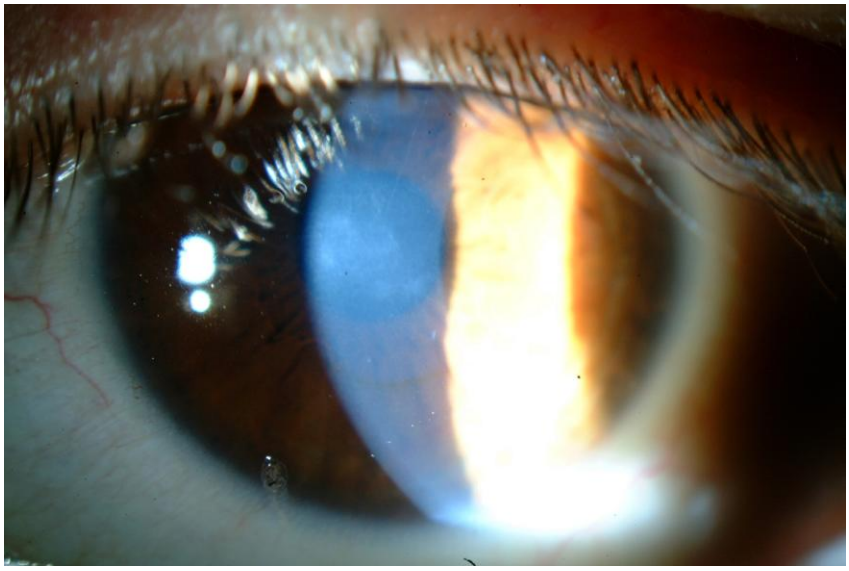

Figure 1. Fleischer's ring, a hemosiderin arc around the cone base (from our own database).

Another characteristic sign is the presence of Vogt's striae (Figure 2), which are fine vertical lines produced by compression of Descemet's membrane, which tend to disappear when physical pressure is exerted on the cornea.

Figure 2. Vogt's striae, fine vertical lines produced by compression of Descemet's membrane (from our own database).

DOI:10.14753/SE.2012.1628

The increased visibility of corneal nerves and observation of superficial and deep corneal opacities are also common signs, which can be present at different severity stages of the disease. The majority of contact lens patients eventually develop corneal scarring. Munson's sign (Figure 3), a V-shape deformation of the lower eyelid when the eye is in downward position, and Rizzuti's sign, a bright reflection of the nasal area of the limbus when light is directed to the temporal limbal area, are signs frequently observed in advanced stages (2,3).

Figure 3. Munson's sign, a V-shape deformation of the lower eyelid when the eye is in downward position (from our own database).

Acute hydrops (Figure 4) is a well-known complication, occurring in approximately 3% of patients with keratoconus. Hydrops occurs after rupture of the posterior cornea leads to an influx of aqueous humor into the cornea, resulting in edema. Corneal edema typically resolves in 6 to 10 weeks; therefore, hydrops is usually not an indication for emergency corneal transplantation (17).

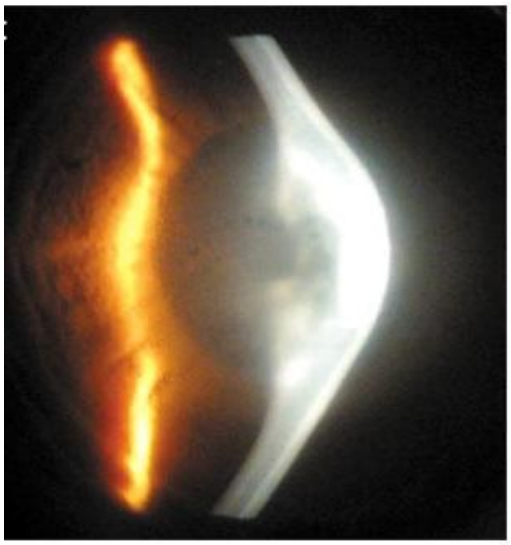

Figure 4. Acute hydrops, rupture of the posterior cornea with a consequent influx of aqueous humor into the cornea (17).

DOI:10.14753/SE.2012.1628

1. 3. Histopathology

Thinning of the corneal stroma, breaks in Bowman's layer, and deposition of iron in the basal layers of the corneal epithelium comprise a triad of the classical histopathologic features found in keratoconus (Fig. 5). Depending on the stage of the disease, every layer and tissue of the cornea can, however, become involved in the pathological process. Fine details of these processes are most clearly appreciated by electron microscopy (2).

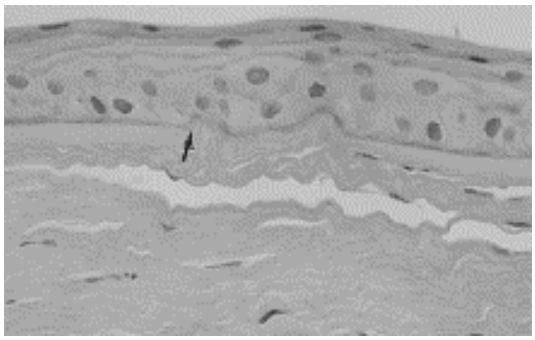

Figure 5. Breaks in Bowman's layer (arrow) (3).

The epithelium may show degeneration of its basal cells, breaks accompanied by downgrowth of epithelium into Bowman's layer, particles within a thickened subepithelial basement membranelike layer and between basal epithelial cells, and accumulation of ferritin particles within and between epithelial cells most prominently in the basal layer of the epithelium. Histopathologic features detected in Bowman's layer may include breaks filled by eruptions of underlying stromal collagen, periodic acid Schiff–positive nodules, and Z-shaped interruptions, possibly due to separation of collagen bundles and reticular scarring. Features noted in the stroma are compaction and loss of arrangement of fibrils in the anterior stroma, decrease in the number of collagen lamellae, normal and degenerating fibroblasts in addition to keratocytes, and fine granular and microfibrillar material associated with the keratocytes.

Descemet's membrane is rarely affected except for breaks seen in acute hydrops. The endothelium is usually normal. However, some abnormalities have been reported, including intracellular "dark structures," pleomorphism, and elongation of cells with their long axis toward the cone. Gross histopathologic analysis of corneal buttons undergoing penetrating keratoplasty for keratoconus has revealed the presence of two types of cone morphology: "nipple"-type cones, located centrally, and "oval"-(sagging) type cones, located inferiorly or inferotemporally. These types of cones often can be distinguished on slit-lamp examination or evaluation of the anterior corneal topography in keratoconus patients (2,3).

DOI:10.14753/SE.2012.1628

Histopathologic examination of corneal buttons in patients who have had acute hydrops reveals stromal edema (Figure 6). Descemet's membrane separates from the posterior surface and retracts into scrolls, ledges, or ridges. During the repair process, corneal endothelium extends over the anterior and posterior surfaces of the detached Descemet's membrane and denuded stroma: endothelial integrity is usually reestablished 3–4 months after the acute event (2-4).

Figure 6. Corneal hydrops and the break in Descemet's membrane with scrolled edges (4).

1. 4. Etiology and Pathogenesis

1.4. 1. Associated disorders

Keratoconus commonly develops as an isolated condition, although it has also been described in association with many syndromes and diseases (2,3,18). Studies have reported that 0.5–15% of subjects with Down's syndrome suffer from keratoconus, leading to an association 10–300 times higher than that of the normal population. This association has been suggested to occur as a result of eye rubbing owing to the increased rate of blepharitis seen in approximately 46% of Down's syndrome individuals (19). It has also been found that 30–41% of subjects with Leber's congenital amaurosis, a rare genetic disorder, also suffer from keratoconus (20). Although keratoconus in Leber's congenital amaurosis has been documented as an oculo-digital sign (i.e., patients rub their eyes with the fingers in a strongly and compulsively manner), genetic rather than eye rubbing mechanisms for keratoconus have also been identified (2,3). Certain studies suggest that keratoconus patients do rub their eyes more often than normal (21). Contact lenses are also suggested as a source of mechanical trauma related to keratoconus (2,3). Because early in the disease process patients have mild myopic astigmatism with clinically normal-looking corneas and their vision is best corrected

with rigid contact lenses, it is extremely difficult to determine which came first, the keratoconus or contact lens wear.

Other associations between keratoconus and connective tissue disorders, such as Ehlers-Danlos syndrome subtype VI, Osteogenesis imperfecta and joint hypermobility have previously been reported (2). Additionally, some studies have found an association between advanced keratoconus and mitral valve prolapse (22).

Atopy is also reported to be highly associated with keratoconus (2,21).

1.4. 2. Biochemical studies

Despite the intensive research activity over the last few decades into the etiology and pathogenesis of keratoconus, the causes and possible mechanisms for its development remain poorly understood. Corneal thinning appears to result from loss of structural components in the cornea, but why this occurs is not clear. Theoretically, the cornea can thin because it has fewer collagen lamellae than normal, fewer collagen fibrils per lamella, closer packing of collagen fibrils, or various combinations of these factors. These conditions may result from defective formation of extracellular constituents of corneal tissue, a destruction of previously formed components, an increased distensibility of corneal tissue with sliding collagen fibers or collagen lamellae, or a combination of these mechanisms (2). Several biochemical theories for keratoconus development have been proposed to support the hypothesis that corneal thinning occurs as a result of the loss of corneal structural components. Määttä et al. found differences in collagen types XIII, XV and XVIII between normal and keratoconic corneas, leading to the suggestion that these differences might play an active role in the wound healing process observed between normal and keratoconic corneas (3,23, 24).

The excessive degradation of the corneal stroma commonly observed in keratoconus might be the result of proteolitic enzyme activity that can be initiated by an increased level of proteases and other catabolic enzymes, or decreased levels of proteinase inhibitors such as α2-macroglobulin and α1-antiprotease (25).

It has also been found that keratocytes in keratoconus have four times greater numbers of Interleukin-1 receptors compared to normal subjects. As Interleukin-1 has been postulated to be a modulator of keratocytes proliferation, differentiation and death, it has been suggested that the loss of anterior stromal keratocytes might occur due to an excess of apoptotic cell death and stromal mass loss. Furthermore, if epithelial microtrauma leads to an increased release of Interleukin-1, the latter provides support towards the association of keratoconus with eye rubbing, contact lens wear and atopy (26).

DOI:10.14753/SE.2012.1628

The different distribution and lower number of stromal lamellae in keratoconic compared with normal corneas and has been proposed as a precursor for corneal rigidity reduction and thinning, ultimately leading to keratoconus development. Furthermore, oxidative damage has been described as a co-factor in keratoconus progression. Keratoconic corneas have decreased levels of aldehyde dehydrogenase Class 3 and superoxide dismutase enzymes. Both of these enzymes play important roles in the reactive oxygen processes of different species. The reactive oxygen accumulation causes cytotoxic deposition of malondialdehyde and peroxynitrites, which could potentially damage corneal tissues. The main factors related to increased oxidative damage are ultraviolet radiation, atopy and mechanical trauma; the latter could occur as a result of chronic eye rubbing and contact lens wear (3, 27, 28).

1.4. 3. Genetics

Although formal genetic analyses using current methodology have not been reported for keratoconus, review of the published literature provides strong pointers to suggest genetic influences in the pathogenesis of this disorder. Several large series have reported a positive family history in 6–10% of patients with keratoconus (3, 21). The majority of reported studies suggested an autosomal dominant mode of inheritance with variable expression and included subtle forms of the disorder, such as keratoconus fruste or mild irregular astigmatism, in order to resolve the mode of inheritance. Although there are several reports in the literature that suggest recessive inheritance, none show clear evidence that three generations were examined or that subtle forms of the disorder were sought for inclusion in the pedigree analysis (2,3, 29, 30). The degree of penetrance was approximately 20%. The disease was characterized by complete penetrance and variable expressivity (31).

Several loci, have been associated to keratoconus disease in different studies. Héon et al. identified four mutations of the VSX1 gene (i.e., R166W, L159M, D144E and H244R) in different keratoconic patients (32). Bisceglia et al. also found four mutations of the VSX1 gene (i.e., D144R, G160D, P247R and L17P) in 7 out of 80 keratoconus subjects assessed (33). Recently, Eran et al. identified the D144E mutation linkage in a Jewish family affected by keratoconus (34). In contrast, Aldave et al. reported that just 2 out of 100 keratoconus subjects showed any gene mutation (35). More recently, Liskova et al. have shown that mutation of D144E is not the direct cause of keratoconus development (36) and Tang et al. have identified that mutations L159M, R166W and H244R are not related to keratoconus (2,37).

DOI:10.14753/SE.2012.1628

Although several previous reports have investigated the genetics of keratoconus, futher analyses are needed to accurately define hereditary patterns for various subtypes of keratoconus and elucidate the role genetic influences may play in its pathogenesis. Formal genetic analyses of a disease or trait are used to test whether there is a significant genetic influence in the etiology of the disease and to identify both the modes of inheritance of any responsible genes and their locations in the human genome. In a genetic analysis, the first question to be investigated is whether familial aggregation is the result of genetic factors (2,3).

1.5. Diagnosis of keratoconus

1.5.1. Photokeratoscopy and keratometry

Several devices are currently available for detecting early keratoconus by measuring anterior corneal topography. The early diagnostic methods were simple inexpensive devices, such as handheld keratoscopes (placido disks). With the hand-held keratoscopes, such as the Klein keratoscope, early keratoconus is characterized by a downward deviation of the horizontal axis of the Placido disk reflection. In 1938 Marc Amsler, using a photographic placido disk, was the first to describe early corneal topographic changes in keratoconus before clinical or biomicroscopic signs could be detected (Figure 7). His classical studies on the natural history of keratoconus documented its progression from minor corneal surface distortions to clinically detectable keratoconus. He classified keratoconus into clinically recognizable stages and an earlier latent stage recognizable only by placido disk examination of corneal topography. These early stages were subdivided into two categories: keratoconus fruste, in which there is a 1–4 degree deviation of the horizontal axis of the placido disk, and early or mild keratoconus, which has a 4–8 degree deviation. Only slight degrees of asymmetric oblique astigmatism could be detected in these early forms. Similar findings were absent in patients with regular astigmatism (38, 39).

DOI:10.14753/SE.2012.1628

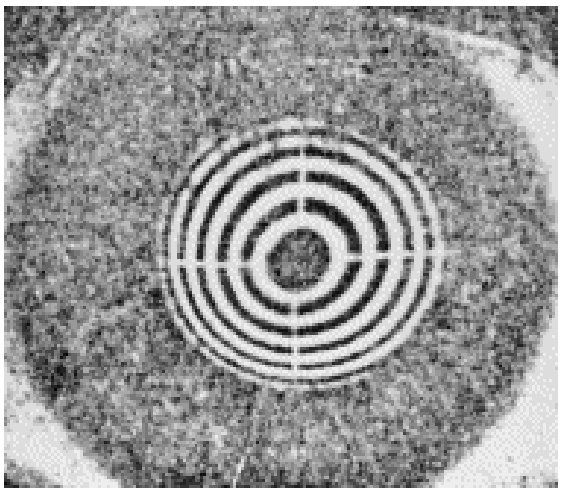

Figure 7. Photographic placido disk images used by Amsler. Deflection of the horizontal meridian labeled as keratoconus (3).

The photokeratoscope produces a topographic record of 55–80% of the total corneal contour, but it provides little or no information about the central 3 mm of the cornea. The ophthalmometer (keratometer), which provides information about only 2–3 points approximately 3 mm apart, can detect keratoconus by showing distortion of its mires or central or inferior steepening. While steep corneas might suggest keratoconus, there are patients with steep corneas and high degrees of regular astigmatism who do not have keratoconus. Conversely, there are patients who have keratoconus with normal central corneal curvatures but irregular astigmatism or inferior steepening only. A documented increase in corneal curvature over time as seen by keratometry is a sensitive indicator of keratoconus (3).

1.5.2. Computer-assisted videokeratoscopy

Computer-assisted videokeratoscopes, which generate color-coded maps and topographic indices, are currently the most widespread devices for confirming the diagnosis of keratoconus. With such devices, keratoconus appears as an area of increased surface power surrounded by concentric zones of decreasing surface power. Three features are common to keratoconus videokeratographs that use sagittal topography, a localized area of increased surface power, inferior-superior power asymmetry, and skewed steep radial axes above and below the horizontal meridian, depicting irregular astigmatism, the hallmark of keratoconus (2-4,7,8).

DOI:10.14753/SE.2012.1628

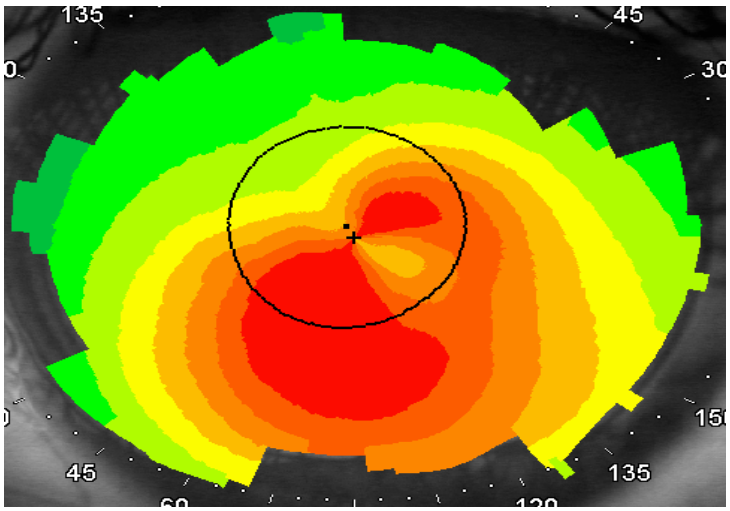

Figure 8. Typical features of keratoconus seen on sagittal topography, a localized area of increased surface power, inferior-superior power asymmetry, and skewed steep radial axes above and below the horizontal meridian (from our own database).

Placido-disk based computer videokeratoscopes, such as the TMS (Topographic Modeling System, Computed Anatomy, New York, NY) , have the combined features of both a keratometer and photokeratoscope, recording curvature changes in both the central and paracentral cornea, they are ideally suited for detecting subtle topographic changes present in early keratoconus and for documenting their progression by serial topographic analysis (40).

Several studies have been performed to characterize the topographic phenotype of clinically detectable keratoconus by videokeratography. The majority of patients have peripheral cones, with steepening extending into the periphery (Figure 8). The steepening in this group is usually confined to one or two quadrants. A smaller group of patients have central topographic alterations. Many central cones have a bow tie configuration similar to that found in naturally occurring astigmatism. In the keratoconus patients, however, the bow tie pattern is asymmetric, with the inferior loop being larger in most instances. In contrast to eyes having with-the-rule astigmatism, the steep radial axes above and below the horizontal meridian in keratoconus appear skewed, giving the bow tie a lazy-eight configuration. Another pattern found in central cones is more symmetric steepening without a bow tie appearance (41, 42). The pattern is usually the same in both eyes, although it may be more advanced in one eye than in the other (3). Figure 9 depicts the typical topographic patterns of keratoconus.

DOI:10.14753/SE.2012.1628

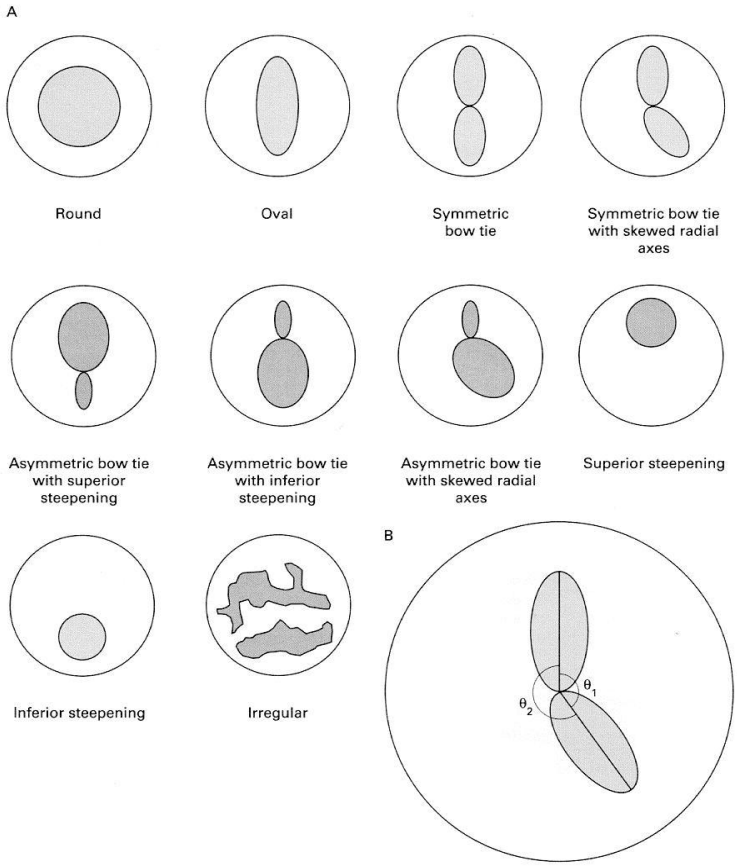

Fig. 9. Classification scheme of normal videokeratographs in the absolute scale devised as a baseline to monitor topographic progression to keratoconus (41).
Top: round, oval, symmetric bow tie and symmetric bow tie (AB) with skewed radial axes.
Middle: asymmetric bow tie with superior steepening, asymmetric bow tie with inferior steepening (IS), asymmetric bow tie with skewed radial axes and superior steepening.
Bottom: inferior steepening, irregular and bow tie with skewed radial axes (AB/SRAX). Lower right figure is a schematic illustration of how to determine whether a pattern is AB/IS or AB/SRAX. A line is drawn to bisect the upper and lower lobes of the asymmetric bow tie (see solid lines), if there is no significant deviation from the vertical meridian (i.e., no skewing), the pattern is designated as AB/IS (as in bottom A); if the lines bisecting the two lobes appear skewed by more than 30° from the vertical meridian (i.e., 150° from one another), it is labeled as AB/SRAX.

Possible sources of confusion in the diagnosis of keratoconus are videokeratography patterns simulating keratoconus (videokeratographic pseudokeratoconus) (3). The most common culprit is contact lens wear (both hard and soft), which induces patterns of inferior steepening that may be very difficult to distinguish from keratoconus (43). These patterns,

however, disappear with time (1-2 month) after contact lens wear is discontinued. Videokeratographic pseudokeratoconus may also result from technical errors during videocapturing, such as inferior eyeball compression, misalignment of the eye with inferior or superior rotation of the globe, and incomplete digitization of mires, causing formation of dry spots, which simulates inferior steepening (2,3).

Developing quantitative descriptors of videokeratography patterns in keratoconus would allow for easier recognition of patterns and enable us to develop a quantitative phenotype that could be universally used to formulate minimal topographic criteria for diagnosing keratoconus. The Smolek-Klyce method results in the keratoconus severity index (KSI), which is obtained with a combination of neural network models and decision tree analysis.36 The KSI increases in a more or less linear fashion with the progression of keratoconus. Thus, this variable can be used to track the natural history of the disease. It is also possible to detect asymptomatic keratoconus when KSI reaches 15%; a KSI of 30% or higher indicates clinical keratoconus (44). The network method accurately classified keratoconus suspect cases and was found to be significandy sensitive and specific for these cases. The severity network established statistically validated numeric thresholds which can be useful to clinically monitor and document cone development (45).

Rabinowitz et al. (46) have developed three indices that distinguished eyes with keratoconus from normals: central K (descriptive of central steepening); I-S values (inferior-superior dioptric asymmetry); and R versus L (difference between right and left central corneal power). These abnormalities were similar to, but less severe than, those found in the patients with keratoconus. It is possible that these indices are descriptive of the earliest stages of keratoconus in normal eyes before they progress to keratoconus, and these abnormalities might represent variable expression of a keratoconus gene in these families. A new index has also been developed that is more specific to keratoconus and that quantifies the irregular astigmatism that typifies the keratoconus videokeratograph, the SRAX index. Corneal topography is considered suspect of keratoconus when it meets the following criteria: central keratometry value >47.2 diopters (D) or inferior minus superior (I–S) average keratometry >1.4 D or KISA% > 60%. (46-47).

Disease detection, even at early stages, has become increasingly important particularly in an attempt to prevent iatrogenic ecstasia formation – the lost of corneal shape – which has been widely documented in patients with subclinical forms of keratoconus who have undergone refractive surgery procedures. For this reason, several, above not mentioned index-based classification methods build on corneal topography systems for grading the severity of keratoconus have been developed.

DOI:10.14753/SE.2012.1628

1.5.3. Elevation based topography

Measurement of Placido-disk based corneal topography and central corneal thickness are widely used methods in the diagnosis of keratoconus, however they are of limited use. Placido-disk based corneal topography only examines the anterior surface of the cornea and alteration in the reference point or viewing angle may result in inaccuracy of curvature measurement (48-51). Ultrasound pachymetry, which is widely used for the measurement of central corneal thickness, is a contact device and precise measurement depends on correct probe alignment and centration (52).

With the advent of Orbscan slit-scanning topography (Bausch & Lomb, Orbtek Inc., Salt Lake City, UT) and the Pentacam Comprehensive Eye Scanner (Oculus, Wetzlar, Germany) anterior and posterior corneal surface elevation data measurement and pachymetry map detection have become possible. Height data give a more accurate representation of the true shape of the corneal surface because they are independent of axis, orientation and position (7,8,48,49). Both the Orbscan and the Pentacam have the advantage of being non-contact methods.

1.5.3.1. Orbscan

Another technique, slit-scanning topography/tomography, scans the entire surface of the cornea; it measures elevation and pachymetric parameters, the ACD, and the anterior chamber angle of the eye. It is based on the principle of measuring the dimensions of a slit‑scanning beam projected on the cornea. Orbscan II and newer versions have a Placido-disc attachment in order to obtain curvature measurements directly. The latest hardware upgrade, Orbscan IIz, can be integrated with a Shack Hartmann aberrometer in the Zyoptix workstation. This integrated system offers total wavefront analysis through the 5th order and identifies the total aberrations of the eye. The Orbscan IIz scans the entire surface of the cornea and acquires over 9000 data points in 1.5 seconds. The curvature of the anterior and posterior surfaces of the cornea can be assessed along with the anterior surface of the lens and the iris. Mapping of the iris in conjunction with posterior surface corneal topography allows an estimation of the iridocorneal angle of the eye. Some studies demonstrated, that Orbscan seemed to underestimate corneal thickness readings in eyes with keratoconus and in eyes after excimer laser keratorefractive surgery (52-57).

DOI:10.14753/SE.2012.1628

1.5.3.2. Scheimpflug camera

Pentacam Scheimpflug uses the Scheimpflug principle in order to obtain images of the anterior segment. The Scheimpflug principle describes the optical properties involved in the photography of objects when their plane is not parallel to the film of the camera. It requires that the plane containing the slit beam and the image plane intersect at one point, with the corresponding angles equal. It has a rotating Scheimpflug camera that takes up to 50 slit images of the anterior segment in less than 2 seconds. Software is then used to construct a three dimensional image. A second camera captures eye movements and makes appropriate corrections. It calculates data for corneal topography (anterior and posterior corneal surface) and thickness, anterior chamber depth (ACD), lens opacification and lens thickness. It allows the measurement of local elevation points by fitting the corneal shape to a best fit sphere reference surface with variable diameters or to an ellipsoid surface. Examination of the posterior corneal surface is important in the early diagnosis of keratoconus as epithelial compensation can mask the presence of an underlying cone on the anterior surface (Figure 10) (56). It also provides data on corneal wavefront of the anterior and posterior corneal surface using Zernike polynomials. A newer version has recently become available, the Pentacam HR. In addition to a higher resolution camera, it has phakic intraocular lens (IOL) software that simulates the position of the proposed lens. The quality of the lens data depends on the pupil size, as only part of the lens can be examined through the pupillary aperture (53,55,58-60). Several studies have evaluated the reproducibility and repeatability of Scheimpflug imaging devices, which have been shown to give reliable corneal thickness measurements in eyes with keratoconus (52,57).

There are few studies of other devices useful for the detection of keratoconus. The most common method for measuring central corneal thickness (CCT) is ultrasound biometry; however, this requires a contact device and precise measurement depends on correct probe alignment and centration. Although US biomicroscopy allows detailed measurement of the cornea and anterior chamber, it also requires contact with the eye (52). Several other methods, including optical coherence tomography, specular microscopy and partial coherence interferometry were recently developed to measure the cornea and anterior chamber (54,57).

DOI:10.14753/SE.2012.1628

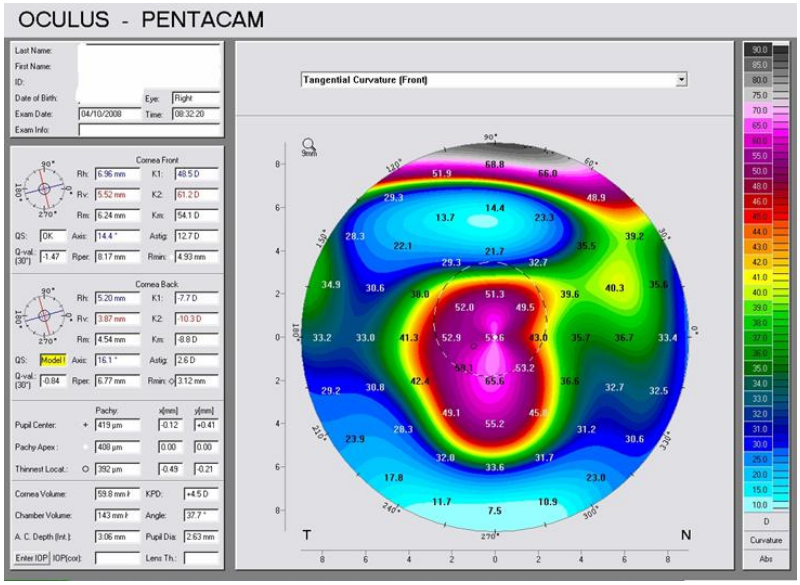

Figure 10. Typical features of keratoconus seen on an anterior elevation map of the Pentacam, an increased positive elevation (65µm) can be seen at the apex of the cone. Keratometric and pachymetric data are depicted at the left side of the image (from our own database).

1.5.4. Wavefront aberrometry

Measurement of Placido-disk based corneal topography and central corneal thickness are currently the most widely used methods in the diagnosis of keratoconus. In more advanced cases this is not complicated, because of the typical biomicroscopic and topographic findings, but the detection of subclinical or forme fruste cases with corneal topography alone may impose difficulty. Understanding the characteristics of ocular higher-order aberrations due to keratoconus might be very useful to differentiate early cases from simple myopia or myopic astigmatism (61,62). Corneal higher-order aberrations in keratoconus have been investigated by several authors. This latter is mathematically calculated from corneal topographic elevation data and does not take into account the internal ocular aberrations. The advantage of measuring corneal aberrations is its ability to analyze most of the anterior corneal surface, it allows a better understanding of the optical behavior of the cornea (63-66).

Aberrometry uses wavefront sensing, which is a technique of measuring the complete refractive status, including irregular astigmatism, of an optical system. Light is defined differently in geometrical and physical optics. In geometrical optics, the rays from a point source of light radiate out in all directions. Light coming from infinity is considered to be

DOI:10.14753/SE.2012.1628

linear bundles of light rays. In physical optics, on the other hand, light is expressed as a wave, and the light waves spread in all directions as a spherical wave. The wavefront is the shape of the light waves that are all in-phase. Light coming from infinity is expressed as proceeding as a plane wavefront. A wavefront aberration is defined as the deviation of the wavefront that originates from the measured optical system from reference wavefront that comes from an ideal optic system. The unit for wavefront aberrations is microns or fractions of wavelengths and is expressed as the root mean square or RMS. The purpose of wavefront analyses of the eye is to evaluate the optical quality of the eye by measuring the shape of its wavefront as wavefront aberrations. For this, an aberrometer or wavefront sensor is used, and for measuring the corneal wavefront aberrations, a corneal topographer is used.

The shape of the wavefront can be analysed by expanding it into sets of Zernike polynomials. The Zernike polynomials are a combination of independent trigonometric functions that are appropriate for describing the wavefront aberrations because of their orthogonality. The first to sixth orders Zernike polynomials are shown graphically in Figure 11. The zero order has one term that represents a constant. The first order has two terms that represent tilt for the x and y axes. The second order includes three terms that represents defocus and regular astigmatism in the two direction. The third order has four terms that represent coma and trefoil, and similarly, the fourth order has five terms that represent tetrafoil, secondary astigmatism and spherical aberration.

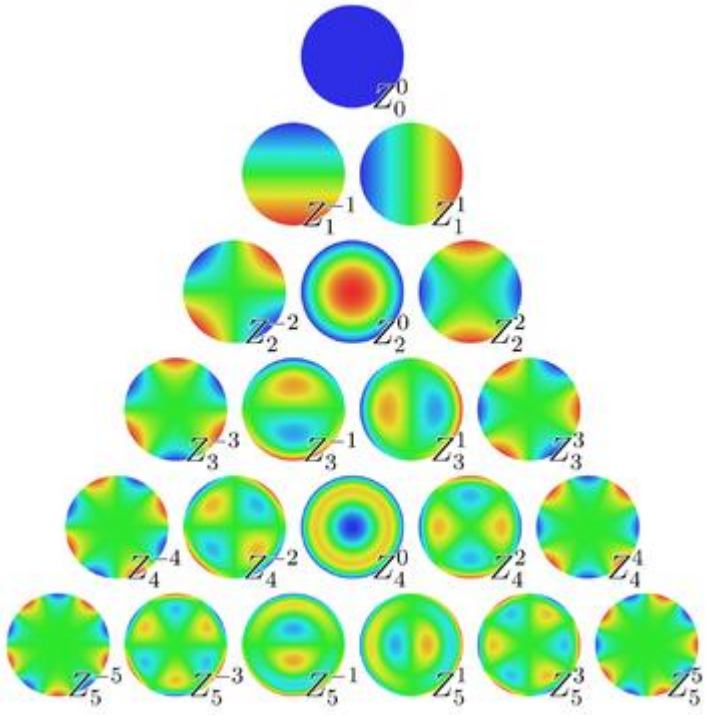

Figure 11. The first to sixth orders Zernike polynomials shown graphically (67).

DOI:10.14753/SE.2012.1628

The polynomials can be expanded up to any arbitrary order if a sufficient number of measurements are made for the calculations. Spectacles can correct for only the second order aberrations, and not the third- and higher-orders that represent irregular astigmatism. Monochromatic aberrations can be evaluated quantitatively using the Zernike coefficients for each term.

Although the total HOAs can be used to estimate the severity of deterioration of optical quality of the eye as the diagnostic purposes, it will be essential for the surgical treatments to quantify the details of wavefront of the eye using Zernike expansion or Fourier expansion.Wavefront aberrations caused by the anterior and/or posterior corneal surfaces can be calculated using the height data of the corneal topographers such as videokeratoscopes or slit-scanning corneal topographers (67).

1.6. Treatment of Keratoconus

1.6.1. Contact lenses

As irregular astigmatism can not be corrected with spectacles, contact lens is the most widly used optical correction method of keratoconus. Although contact lenses for keratoconus are manufactured with hydrogel, silicone hydrogel, gas permeable and hybrid (i.e., rigid centre and soft skirt) materials, gas permeable contact lenses remain the most commonly used contact lens type, as high levels of irregular astigmatism cannot normally be corrected with other contact lens types. Piggy back systems, consisting on the fitting a gas permeable on top of a soft contact lens, have also been used for keratoconus management. The soft contact lens is used to improve wearing comfort and provide a more regular area for the gas permeable contact lenses to sit, whereas the gas permeable contact lens is primarily used for providing adequate visual acuity. The use of high oxygen permeability soft (i.e., silicone hydrogel) and gas permeable contact lenses is highly recommended for keratoconus management as these corneas are well known to be compromised (2, 71-73).

DOI:10.14753/SE.2012.1628

1.6.2. Corneal crosslinking

Crosslinking is a widespread method in the polymer industry to harden materials and also in bioengineering to stabilize tissue. Using UVA at 370 nm and the photosensitizer riboflavin the photosensitizer is excited into its triplet state generating so-called reactive oxygen species (ROS) being mainly singlet oxygen and to a much lesser degree superoxide anion radicals. The ROS can react further with various molecules inducing chemical covalent bonds bridging amino groups of collagen fibrils. The wave length of 370 nm was chosen because of an absorption peak of riboflavin at this wavelength (74,75).

The first clinical study on the crosslinking treatment of keratoconus was performed by Wollensak. In this 3-year study, 22 patients with progressive keratoconus were treated with riboflavin and UVA. In all treated eyes, the progression of keratoconus was at least stopped (‘freezing’). In 16 there was also a slight reversal and flattening of the keratoconus by two diopters. Best corrected visual acuity improved slightly in 15 eyes (74).

Crosslinking treatment of keratoconus is a very promising new method of treating keratoconus. At the present stage of knowledge, the treatment should only be performed in patients with documented progression of keratoconus in the preoperative months. With more long-term experience, prophylactic treatment of keratoconus at an early stage might become possible. Additional refractive corrections can also be considered if necessary. In case a recurrence of keratoconus progression should occur in the long run, which has not been observed so far, a second crosslinking procedure might be a choice.

However safe and promising technik CXL is, the proper determination of inclusion criteria may significantly reduce the complications and failures. A preoperative maximum K reading less than 58.00 diopters may reduce the failure rate to less than 3%, and restricting patient age to younger than 35 years may reduce the complication rate to 1% (76). As postopertiv complication stromal infiltrations and moderate anterior chamber inflammation has been described and diffuse lamellar keratitis (DLK) after myopic laser in situ keratomileusis. Herpes simplex keratitis and iritis recurrence has been also associated with the intervention (76).

1.6.3.1. Surgical interventions: ICRS

Intrastromal corneal ring segments (ICRS) were initially developed for the correction of mild to moderate myopia and are now considered in the management of keratoconus and

other ectatic disorders, such as ectasia after laser in situ keratomileusis and pellucid marginal degeneration. The ICRS acts as a passive element that flattens the central cornea by an arc-shortening effect on the corneal lamellae structure (Figure 12). Although ICRS implantation is an effective tool in managing corneal ectatic disease, several complications have been described. These include incomplete tunnel creation, anterior or posterior corneal perforation, epithelial defects, segment extrusion, and induced astigmatism by central migration of the ICRS along the horizontal corneal diameter. In most of these cases, ICRS explantation is mandatory and it is possible that a more appropriate ICRS can be implanted later. A main advantage of ICRS implantation is its potential reversibility because the technique does not require tissue removal; this has been shown in eyes with low to moderate myopia.

The outcomes of corneal remodeling by ICRS are mainly dependent on the biomechanical properties of the corneal tissue. The corneal response depends on the magnitude of the force and on the velocity of the application of the force. A specific ICRS inducing a specific force on the cornea will generate different changes in the ectatic corneal profile, depending on the underlying corneal biomechanical status. Theoretically, the cornea should have the ability to return to its original state after removal of the application of force. In addition, it should be able to be remodeled when new forces are applied (ie, after implantation of a new ICRS). (77,78).

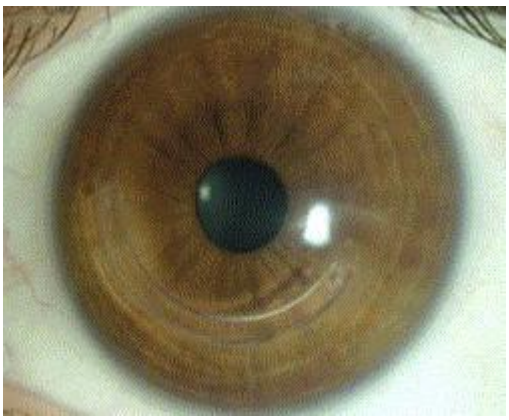

Figure 12. Clinical picture of an after ICRS implantation (79).

1.6.3.2. Surgical interventions: keratoplasty

The refractive error caused by the ectatic cornea is initially managed with either spectacles or contact lenses. When ectasia progresses to the point where contact lenses no longer provide useful vision, then surgical intervention may be considered. Penetrating keratoplasty is the most commonly performed surgical procedure for ectatic corneas, but is associated with complications including graft rejection, induced astigmatism, complications

of intraocular surgery such as glaucoma, cataract formation, retinal detachment, cystoid macular edema, endophthalmitis, and expulsive hemorrhage. To avoid these complications, new methods such as lamellar keratoplasty (LKP) have evolved. LKP has the advantages of being extraocular and reversible if tissue complications occur. Another advantage includes the ability to replace only selected areas of diseased corneal tissue with healthy donor tissue. LKP results, however, may be limited by vision-reducing graft-host interface problems and the technical nature of the surgical procedure (80,81). In keratoconus, conventional penetrating keratoplasty has long been associated with good long-term outcomes with graft survival of over 90% up to 13.8 years postoperatively. Visual outcomes have also been good with 73.2% achieving BCVA over 20/40 (82,83).

Replacing weakened corneal tissue by corneal transplantation provides a permanent means of substituting, or augmenting of weakened corneal tissue, and the various forms of keratoplasty for ectatic corneal disease may be largely divided into penetrating or lamellar keratoplasty procedures, and central or peripheral keratoplasty procedures according to the precise site of tectonic weakness of the cornea. Recent innovations in lamellar keratoplasty address issues in the management of corneal ectasia. Nevertheless, corneal endothelial replacement is generally unnecessary in keratoconus, which is primarily a corneal stromal disorder, and as the major causes of long-term graft failure and attrition are endothelial in nature, an anterior lamellar keratoplasty approach to keratoconus which avoids unnecessary replacement of normal recipient endothelium is ideal. Penetrating keratoplasty has in the past been associated with better postoperative vision, due in part to the problem of interface haze and irregularities in lamellar keratoplasty (84).

New automated surgical technologies in anterior segment surgery, which have largely been developed for corneal refractive surgery, are now being utilized in keratoplasty surgery, and are able to partially substitute for conventional manual surgical procedures, providing greater precision and reproducibility in lamellar corneal dissection. These include an automated microkeratome-assisted lamellar keratoplasty device and femtosecond laser-assisted lamellar keratoplasty (85).

DOI:10.14753/SE.2012.1628

1.7. Other diseases affecting biomechanical properties of the cornea

1.7.1. Pellucid marginal degeneration

Pellucid marginal degeneration (PMD) is characterized by a peripheral band of thinning of the inferior cornea from the 4 to the 8 o'clock position. There is 1–2-mm uninvolved area between the thinning and the limbus. The corneal protrusion is most marked above the area of thinning, and the thickness of the central cornea is usually normal. Like keratoconus, pellucid marginal degeneration is a progressive disorder affecting both eyes, although eyes may be asymmetrically affected. In moderate cases it can easily be differentiated from keratoconus by slit-lamp evaluation because of the classical location of the thinning. In early cases the cornea may look relatively normal, and in advanced cases it may be difficult to distinguish from keratoconus because the thinning may involve most if not all of the inferior cornea. In both instances videokeratography is very useful to make the distinction. The videokeratograph has a classical "butterfly" appearance (Figure 13), demonstrating large amounts of against-the-rule astigmatism (2-4).

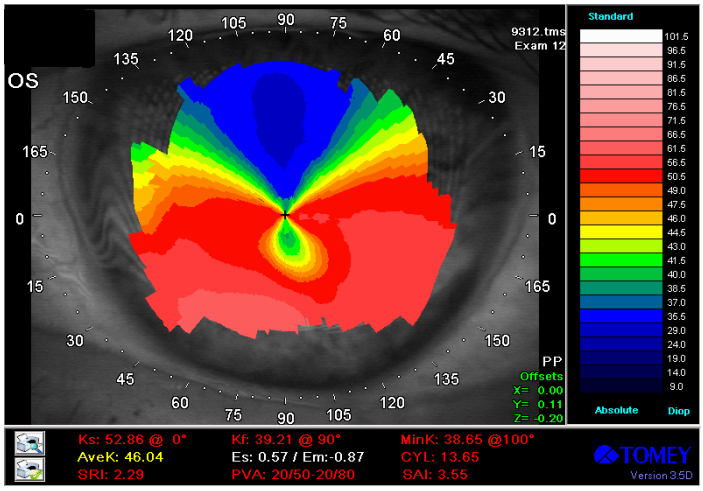

Figure 13. Corneal topography of a patient with PMD. The classical "butterfly" appearance can be clearly seen on the axial map (from our own database).

Pellucid marginal degeneration can be differentiated from other peripheral corneal thinning disorders, such as Terrien's marginal degeneration, because the area of thinning is always epithelialized, clear, avascular, and without lipid deposition. Terrien's corneal degeneration affects a similar age group and also causes high astigmatism; however, it may affect both the superior and inferior cornea and is accompanied by lipid deposition and

DOI:10.14753/SE.2012.1628

vascular invasion. Videokeratography can also be used to differentiate these two disorders because they have distinctly different topographic patterns (86).

Because of the large amounts of against-the-rule astigmatism, patients with pellucid marginal degeneration are much more difficult to fit with contact lenses than patients with keratoconus, although spherical or aspheric contact lenses with large overall diameter should initially be attempted in early-to-moderate cases. Surgery may be considered for patients whose vision is not adequately corrected by contact lenses or in patients who are contact lens-intolerant. Patients with pellucid marginal degeneration, however, are typically poor candidates for penetrating keratoplasty for two reasons. First, thinning occurs so near the limbus that the donor cornea must be placed very close to the corneal limbus, thus increasing the chances of graft rejection. Second, because of the extreme thinning and the location of the thinning, penetrating keratoplasty typically induces large amounts of postoperative astigmatism, which may be extremely difficult to correct because of disparity in graft-host thickness.

Crescentic lamellar keratoplasty is a useful initial surgical procedure in patients with pellucid marginal degeneration. This procedure involves removing a crescentic inferior layer of ectatic tissue by lamellar dissection and replacing it with a thicker lamellar donor graft. This will, in most cases, eliminate large amounts of against-the-rule astigmatism. In some cases, the patient may become contact lens-tolerant, thus obviating a full-thickness procedure (87).

1.7.2. Keratoglobus

Keratoglobus is a rare disorder in which the entire cornea is thinned most markedly near the corneal limbus, in contrast to the localized thinning centrally or paracentrally in keratoconus. The cornea may be thinned to as little as 20% of normal thickness, and it assumes a globular shape. In advanced keratoconus, the entire cornea can also be thinned and globular-shaped, making it difficult to distinguish these two entities. However, even in very advanced keratoconus there may be a small area of uninvolved cornea superiorly that approaches normal corneal thickness (2-4).

Keratoglobus is bilateral, but it is usually present from birth and tends to be nonprogressive. It can be distinguished from megalocornea and congenital glaucoma because the cornea is usually of normal diameter. It is a recessive disorder and is often associated with blue sclerae and other systemic features, in contrast to keratoconus, which is most commonly an isolated disorder. In contrast to keratoconus, the corneas in keratoglobus are prone to

DOI:10.14753/SE.2012.1628

corneal rupture from even minimal trauma. Thus, hard contact lenses are contraindicated and protective spectacles should be strongly encouraged. If the cornea is extremely thin, a tectonic limbus-to-limbus lamellar keratoplasty should be considered to strengthen the cornea. A subsequent central penetrating keratoplasty may be considered if adequate visual rehabilitation cannot be achieved with glasses (88).

1.7.3. Post-LASIK ectasias

Corneal ectasia after LASIK is a progressive corneal steepening, usually inferiorly, with an increase in myopia and astigmatism, loss of uncorrected visual acuity, and often loss of best-corrected visual acuity that can present days to years after LASIK. The actual incidence remains undetermined, and no good data support firm predictions; previous estimates, however, have ranged from 0.04% to 0.6%. Among members of the International Society of Refractive Surgery (ISRS) of the American Academy of Ophthalmology (AAO) responding to the practice patterns survey in 2004, more than 50% had at least one case of ectasia develop in their practice. Approximately 50% of cases present within the first 12 months, but late onset ectasia can also occur (89).

Corneal refractive surgery alters the effective shape, thickness, curvature, and tensile strength of the cornea. The specific mechanisms resulting in post-LASIK ectasia remain undetermined, although complex biomechanical modeling that takes into account factors such as corneal plasticity and viscoelasticity and corneal parameters such as Young's modulus, Poisson's ratio, and curvature radius, among others, may provide insight in the future (90).

LASIK inevitably reduces the tensile strength of the cornea. Among the first four reported cases, all had greater than 10 diopters of myopia preoperatively and less than 250 μm residual stromal bed thickness (RSB) postoperatively, and two patients had forme fruste keratoconus. According to recommendation a RSB of at least 250–300 μm be maintained to prevent corneal ectasia after myopic keratomileusis (91).

Most authors recognize preoperative topographic abnormalities as uniquely indicative of increased risk for post-LASIK ectasia; the definition of ‘abnormal’, however, remains a source of great debate. Forme fruste keratoconus as defined by the Rabinowitz criteria is a risk factor for post-LASIK ectasia. Pellucid marginal corneal degeneration suspects are also at increased risk. Based on extensive review of the literature, the members of the American Society of Cataract and Refractive Surgery (ASCRS) joint committee now recommend avoiding Lasik in patients with asymmetric inferior corneal steepening or asymmetric bowtie patterns with skewed steep radial axes above and below the horizontal meridian (92).

DOI:10.14753/SE.2012.1628

2. Purposes

1. Currently the diagnosis of keratoconus is based on biomicroscopic findings, corneal topography and ultrasound pachymetry. Placido-disk based corneal topography only examines the anterior surface of the cornea and alteration in the reference point or viewing angle may result in inaccuracy of curvature measurement. Height data give a more accurate representation of the true shape of the corneal surface because they are independent of axis, orientation and position. The Pentacam Comprehensive Eye Scanner uses a rotating Scheimpflug camera and measures both anterior and posterior corneal surfaces by an elevation based system. It allows the measurement of local elevation points by fitting the corneal shape to a best fit sphere reference surface with variable diameters or to an ellipsoid surface. Examination of the posterior corneal surface is important in the early diagnosis of keratoconus as epithelial compensation can mask the presence of an underlying cone on the anterior surface. The purpose of our first study (I) was to evaluate the discriminating ability of pachymetric and elevation data obtained by Pentacam and to rank them according to their usefulness in the differential diagnosis of keratoconus.

2. The purpose of the second study (II) was to find the anterior chamber characteristics of mild keratoconus with the aid of the rotating Scheimpflug imaging and to evaluate trends in corneal protrusion progression. We also aimed to demonstrate that morphological alterations of the cornea are accompanied by localized anterior chamber changes.

3. Understanding the characteristics of ocular higher order aberrations owing to keratoconus might be very useful to differentiate early cases from simple myopia or myopic astigmatism. It is particularly important to detect the disease among refractive surgery candidates, because keratorefractive procedures may worsen their condition. Corneal higher order aberrations are calculated from corneal topographic elevation data and do not take into account the internal ocular aberrations. The advantage of measuring corneal aberrations relates to their ability to analyze most of the anterior corneal surface, which allows a better understanding of the optical behavior of the cornea. The limitation of this method is that it neglects the pupil area and position and it is not aligned to the line of sight (LoS), which is the most relevant reference axis for defining retinal image quality at the point of fixation. The purpose of our third study (III) was to prove our hypothesis that keratoconus causes a shift in the LoS, which acts as a compensating mechanism for increased corneal higher order aberrations. To test our hypothesis, we examined location of the LoS, its position relative to the pupil center, and their impact on ocular higher order aberrations in keratoconic and control

DOI:10.14753/SE.2012.1628

eyes. Taking into account the changes of the LoS allows a better understanding of the pathologic optics of keratoconus, and may have a beneficial effect on increasing the precision of correcting higher order aberrations. According to our knowledge, no such comparisons were performed in previous articles.

DOI:10.14753/SE.2012.1628

3. Methods

3.1. Demographic data

In the first and second studies (I, II) forty-one eyes of 24 patients with mild to moderate keratoconus were included. In the control group, 70 eyes of 41 refractive surgery candidates were included. Among the forty-one eyes with keratoconus 18 patients had binocular keratoconus, 2 patients had unilateral disease, in 3 patients the fellow eye has already undergone penetrating keratoplasty. The control group consisted of 41 normal individuals, of 29 patients both eyes could be evaluated, of 12 patients only one eye could be included in the study, because of previous refractive surgery or corneal disease of the fellow eye. Table 1.A. shows the patients' demographic data. There were no statistically significant differences between the keratoconus and the control groups in age or sex distribution ($p>0.05$).

Table 1.A. Demographic features of the patients (I-II), difference statistically significant ($p<0.05$)

	Subjects	Eyes (n)	Age (y) mean±SD	Gender (M/F)
Keratoconus	24	41	38.7±14.1	15/9
Controls	41	68	40.2±15.1	24/17
p			0.61	0.21

Table 1.B. Demographic features of the patients (III), difference statistically significant ($p<0.05$)

	Subjects	Eyes (n)	Age (y) mean±SD	Gender (M/F)
Keratoconus	30	50	31.5±8.2	13/17
Controls	50	100	30.3±10.9	22/28
p			>0.05	>0.05

In the third study (III) (Table 1.B.) fifty-five eyes of 30 patients with mild to moderate keratoconus and 100 eyes of 50 refractive surgery candidates with normal corneas were included**.** Among keratoconus patients, 25 had binocular keratoconus, 2 patients had unilateral disease, in 3 patients the fellow eye has already undergone penetrating keratoplasty. The control group consisted of 100 healthy eyes of 50 refractive surgery candidates. There were

DOI:10.14753/SE.2012.1628

no statistically significant differences between the keratoconus (mean age: 31.5±8.2 years, 13 men, 17 women) and the control groups by Mann–Whitney nonparametric test (mean age: 30.3±10.9 years, 22men, 28 women) in age or sex distribution (p=0.1).

3.2. Patient inclusion criteria

Both eyes of every patient have undergone a complete ophthalmologic evaluation including slit-lamp biomicroscopy, keratometry, retinoscopy, ophthalmoscopy and Placido-disk based videokeratography. Keratoconic patients included in the study were either mild or forme fruste cases. The criteria for diagnosing keratoconus were defined as the existence of central thinning of the cornea with Fleischer ring, Vogt's striae or both by slit-lamp examination. Forme fruste keratoconus was diagnosed when an abnormal, localized steepening was observed by corneal topography without any slit-lamp findings.

Both eyes of every subject were used in the study, except for those with previous ocular surgery, trauma or other pathology. Control subjects were age matched and had a refractive error of less than ± 5 spheric diopters, and/ or astigmatism less than 3 diopters. Patients who wear rigid contact lenses, were asked to stop using them for 4 weeks, and soft contact lenses were ceased for at least one week before assesment.

From all patients, informed consent was obtained after the characteristics of the study was explained. A review by the local ethics committee was not required. For all study procedures, the tenets of the declaration of Helsinki were followed.

3.3. Patient exclusion criteria

Subjects with corneal scarring, previous ocular surgery, trauma or any other ocular diseases except for keratoconus and refractive errors were excluded from the study.

DOI:10.14753/SE.2012.1628

Severe cases were excluded, because of potential stromal haze or scar formation, which may alter the optical transparency of the cornea and image acquisition of the Pentacam.

3.4. Corneal topographic measurements

Corneal topographic measurement were taken with the Tomey corneal topographer (Tomey Topographic Modeling System software version-4, Tomey Corp, Nagoya, Japan). Both topographic and wavefront aberration images were taken at 5 to 10 seconds after a complete blink, when the tear film layer is the most stable (93).

3.5. Pentacam measurements

All eyes were examined with the Pentacam HR (Oculus Inc.), used by three trained examiners. The readings were taken as recommended in the instruction manual. Briefly, the patients were instructed to keep both eyes open and fixate on the black target, in the center of the blue fixation beam. After attaining perfect alignment, the instrument automatically took 25 Scheimpflug images within 2 seconds. For each eye one high quality image was recorded. In the first study (I) the following data were then exported to a Microsoft Excel spreadsheet: keratometry values in the flat (K_1) and steep (K_2) meridian, corneal astigmatism (cylinder), corneal thickness at the center (central pachymetry) and at the thinnest point of the cornea (minimal pachymetry), the distance of the thinnest point of the cornea (apex of the cone in keratoconic patients) from the center of the cornea in the vertical meridian (y) and local elevation (anterior elevation, posterior elevation) values. For height data measurement, the best fit sphere (BFS) was used as a reference body, using the float option over a 9 mm fit. The float map means, that the reference body has no fixed center, the distance between the cornea and the sphere surface is optimized to be as small as possible. Elevation maps show the difference in height between cornea and reference body, their value is positive, when the measured point of the cornea is above the reference body, and negative, when it lies below. Anterior and posterior elevation data were read as the maximum values above the BFS in the central 5 mm of the cornea.

In the second study (II) the following data were exported for further analysis: the ACD measured from the posterior corneal surface centrally, the ACD at the thinnest point of the cornea, and the ACD 1.0 mm, 2.0 mm, and 3.0 mm inferior–paracentral. For local posterior

DOI:10.14753/SE.2012.1628

elevation measurements, a toric ellipsoid was used as a reference body. The elevation maps from the device show the difference in height between the cornea and reference body; the value is positive when the measured point of the cornea is above the reference body and negative when it is below. Posterior elevation data were read as the maximum values above the toric ellipsoid surface in the central 5.0 mm of the cornea, which in the keratoconus eyes in this study was at the thinnest point of the cornea. The mean keratometry values and the smaller of the 2 chamber angles in the horizontal section calculated from the 3-dimensional model were also determined and processed for analysis.

3.6. Hartmann-Shack aberrometry measurements

All eyes were examined with the WASCA Hartmann-Shack wavefront sensor (Carl Zeiss Meditec AG, Jena, Germany) used by three trained examiners (III). The readings were taken as recommended in the instruction manual. Briefly, the patient positions his or her head on a chin rest and fixates on the center of a circular grid, which is optically fogged. The fixation target and the probe beam were coaxial, located at infinity in order that the retinal image of the narrow probe beam will remain centered on the retinal image of the fixation target (94). The operator manually aligns a reference box on a video monitor with the pupil. This comprises a set of six symmetrical infrared diodes, which are seen as reflections off the corneal surface on the control monitor. The anterior-posterior focus point of measurement is determined by bringing into focus these corneal reflexions. This is achieved by first moving the instrument towards the patient and slowly drawing it back until the optimal focus is found. Measurements are taken until the criteria of measurement selection are met. These are: 1, the CCD spot array is perfectly centered within the reference box both horizontally and vertically. 2, to ensure that there is no, or as little as possible, missing data within the analysis zone (95). Wavefront aberration measurements were standardized to a 4.5 mm pupil. We used no dilating drop, as the aberration profile of a pharmacologically dilated pupil is less relevant to the natural pupil view normally experienced by the patient and in order to avoid instrument myopia (96). Wavefront measurements were performed in a dark room. We used the right-hand coordinate reference frame and the double-index convention for naming the Zernike coefficients and polynomials recommended by the OSA/VSIA Standards Taskforce (97,98). The signs of bilaterally asymmetrical Zernike coefficients of the left eyes affected by enantiomorphism were reversed in order to allow comparison between right and left eyes (99).

DOI:10.14753/SE.2012.1628

The following data were then exported to a Microsoft Excel spreadsheet: average and the steep keratometry values and the axis of the steepest meridian, measured by corneal topography, Root mean square (RMS), higher-order RMS (HORMS) (μm), values of Zernike polynomials up to the sixth-order (μm) and the distance of LoS relative to the pupillary axis given by the aberrometer as x and y offset (mm) values.

To calculate the axis of the LoS relative to the pupil center, vector analysis following the recommendations of the Astigmatism Project Group of the American National Standards Institute and the method suggested by Alpins was applied (100,101). Figure 14 shows the design of vector analysis. The WASCA aberrometer gives the parameters of x and y offsets in mm as the distance of the center of the pupil from the point of reference, the LoS. The angle α was calculated using trigonometrical analysis by equation: tangent α=x/y. The angle α was added or subtracted from the 90° or 270° meridian according to the sign of the x and y offset values. If both x and y had a negative sign (this is the case represented in Figure 15), the angle α was subtracted from the 270° meridian. If both x and y had a positive sign, the angle α was subtracted from the 90° meridian. When x was negative and y positive, the angle α was added to the 90° meridian, when x was positive and y negative, the angle α was added to the 270° meridian. Than the vector was reversed by 180 degrees in order to get the distance of the LoS relative to the pupil center. In order to calculate the distance between the LoS and the pupil center we used Pythagora’s rule.

DOI:10.14753/SE.2012.1628

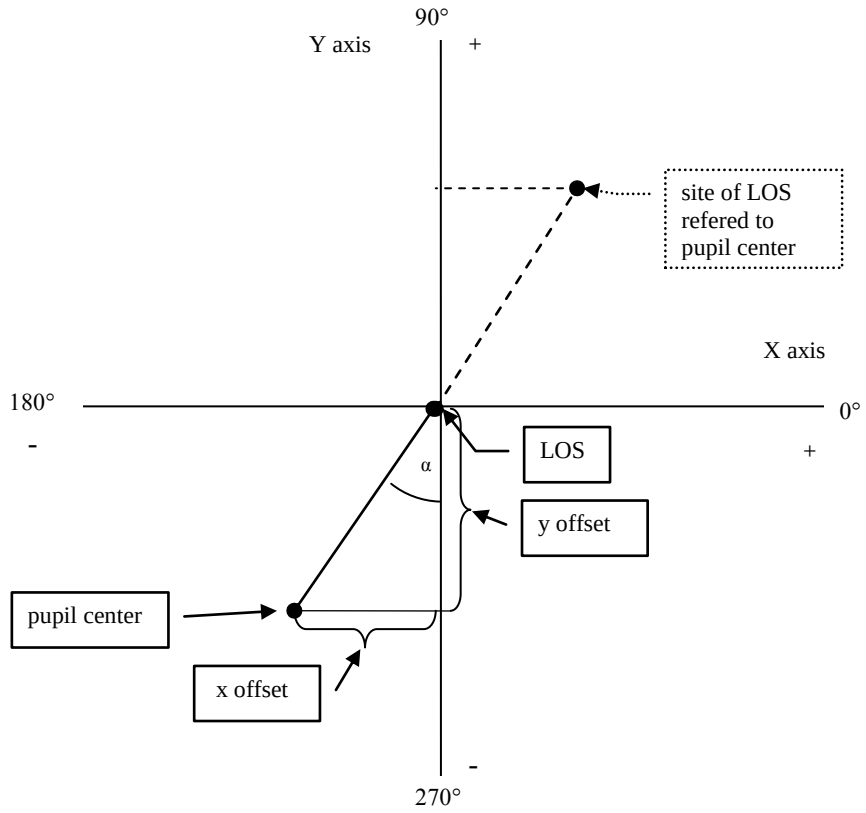

Figure 14. Design of vector analysis. The angle α was added or subtracted from the 90° or 270° meridian according to the sign of the x and y offset values. If both x and y had a negative sign. See further explanation in text.

DOI:10.14753/SE.2012.1628

3.7. Statistical analyses

Statistical analyses were performed with Statistica 8.0 software (StatSoft Inc., Tulsa, OK, USA). Receiver operating characteristic (ROC) curves were obtained using SPSS 15.0 (SPSS Inc., Chicago, Il, USA) (I-III). Normal distribution assumption could not be accepted for anterior elevation according to the Shapiro-Wilks' W test. For group comparisons of continuous variables the Mann-Whitney nonparametric test was used. A p value less than 0.05 was considered statistically significant. Area under the ROC curve (AUROC) was calculated to describe the predictive accuracy of the different indices and to determine the cutoff point for the most sensitive parameter. Logistic regression analysis was performed to investigate predictors of classical topographic and central pachymetric findings contrasted with keratometric, pachymetric and elevation data obtained by the Pentacam with calculation of r^2, positive and negative predictive values. Confirmatory factor analysis (CFA) was performed in the keratoconic group for quantification of the validity of parameters characterizing the disease. CFA is a commonly used statistical method to detect responsible latent factors for the measurable clinical variables which is becoming more and more popular in ophthalmologic research[23]. Briefly, during CFA the most representative variables can be determined using correlation matrices without incorporating any gold standard, and several model structures can be examined. During our analysis different models (with two- and three latent factors) based on our previous assumptions on clinical manifestations of the disease were tested and the best fitted model was chosen by values of fit-indices.

Multivariable regression analysis using a generalized estimating equation (GEE) was performed to determine predictors of keratoconus; data from the eyes were statistically analyzed as repeated measures (102). Thus, the analysis took into account the correlated nature of data from patients who had measurements in both eyes. The construction of the multivariable logistic regression model started with variables that showed the best fit to data in univariable modeling, assessed using the value of the corrected quasi-likelihood under independence model criterion (QICC). Lower QICC values indicate a better fit to data. Next, variables were added and the change in the QICC value was tested. Variables were kept in the model if they were associated with a P value less than 0.05 and the overall fit of the model improved, as indicated by a decrease in the QICC value compared with the value in a model that did not include the variable (58).

Correlations between posterior elevation and corneal protrusion (ACD at minimum pachymetry) were tested using linear and linear piecewise (segmented) regression analysis. Linear piecewise regression analysis models data to identify potentially meaningful trends.

DOI:10.14753/SE.2012.1628

Breakpoints are independent-variable values at which the slope of the linear function changes. Breakpoint values are unknown and are estimated. A nonlinear least-squares regression technique was used to fit the model to the data, and the significance of the breakpoint and the regression coefficients of the slopes were determined. The accuracy of fit of the piecewise regression model was then compared with that of the linear regression model using the explanation coefficients and Akaike Information Criterion (AIC) values of the 2 models. Higher explanation coefficients and lower AIC values indicate that the given regression model is more likely.

Bootstrap method was used to overcome the correlated nature between eyes of the same subject by treating each subject as a cluster (103). Normal distribution assumption could not be accepted for most of the Zernike polynomials according to the Shapiro-Wilks' W test. For group comparisons of continuous variables the Mann-Whitney nonparametric test was used. To test correlations the Spearman rank correlation was used. Factorial regression analysis was used to test the interactive effects of higher order aberrations on the extent of LoS shift. A p value less than 0.05 was considered statistically significant.

DOI:10.14753/SE.2012.1628

4. Results

4.1. Evaluation of elevation parameters of keratoconus with Pentacam (I)

Forty-one eyes of 24 patients with mild to moderate keratoconus were included in the study. In the control group, 70 eyes of 41 refractive surgery candidates were included. Table 2 shows the mean ± standard deviation values of K_1, K_2, cylinder, central and minimal pachymetry, anterior and posterior elevation and y offset in the keratoconic and the control groups. All parameters were statistically significantly different between the two groups ($p<0.001$).

Table 2. Keratometric, pachymetric and elevation parameters of keratoconic and normal corneas, difference statistically significant ($p<0.05$)
K_1=flat keratometry; K_2= steep keratometry; cyl.= cylinder; centr. pachy.= central cornea pachymetry; min.pachy.= minimal pachymetry; ant. elev.= anterior elevation; post. elev.= posterior elevation; y offset value=vertical difference between the vertex normal and the thinnest point of the cornea

Parameter	Keratoconus mean±SD	Control mean±SD	p
K_1 (D)	46.5±4.8	42.8±1.2	<0.001
K_2 (D)	50.2±5.7	43.9±1.5	<0.001
cyl. (D)	3.5±2.7	1.1±0.8	<0.001
centr.pachy. (µm)	491.3±43.5	555.8±27.9	<0.001
min. pachy. (µm)	464.9±54.9	553.1±28.4	<0.001
ant. elev. (µm)	33.3±28.6	2.7±2.3	<0.001
post. elev. (µm)	55.8±33.2	5.7±5.5	<0.001
y (mm)	0.607±0.3	0.208±0.3	<0.001

DOI:10.14753/SE.2012.1628

Figure 15 compares the results of the ROC curve analysis for each parameter; to reduce the number of variables the average values of flat and steep keratometry were included. The graphs show, that posterior elevation has the highest sensitivity in discriminating keratoconus from normal subjects.

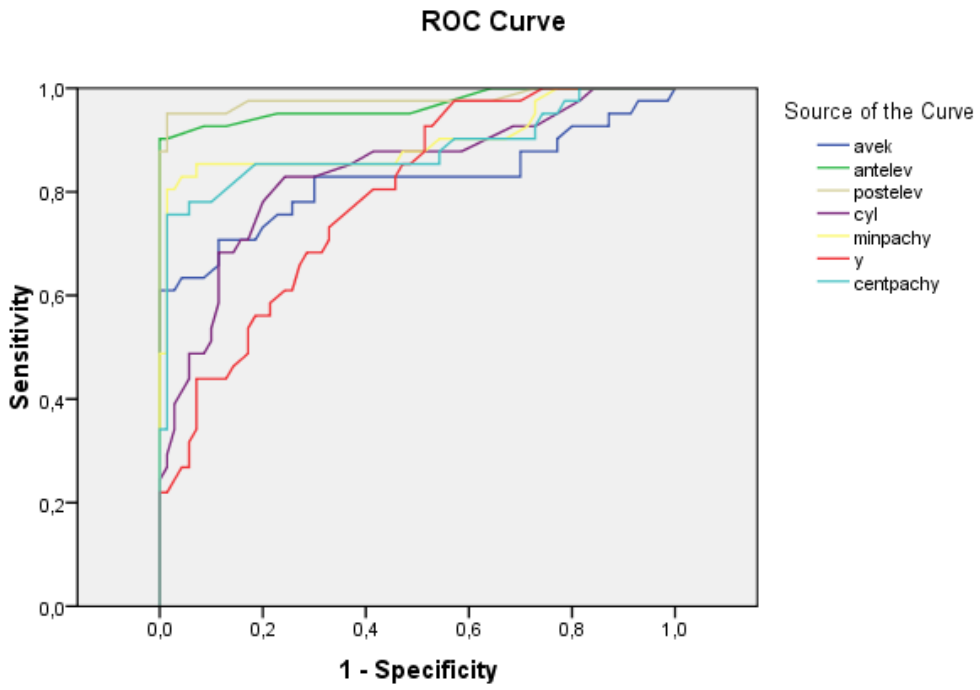

Figure 15. ROC graph showing the sensitivity and specificity of the various corneal measures. The closer the line to the left-hand side of the graph, the higher the sensitivity and specificity for keratoconus.

Table 3 shows that the area under the curve is acceptable for all parameters. Posterior elevation has the highest area under the curve (0.97), followed by anterior elevation (0.96), minimal pachymetry (0.89), central pachymetry (0.88), cylinder (0.83), average keratometry (0.82), and y offset (0.79). ROC analysis result of the x offset value was not acceptable. A posterior elevation cutoff value of 15.5 µm had 95.1% sensitivity and 94.3% specificity in discriminating keratoconus from normal eyes.

DOI:10.14753/SE.2012.1628

Table 3. Area under the curve, standard error and p values of various parameters (keratoconic vs normal eyes).
aveK= average keratometry; cyl.= cylinder; centr. pachy.= central cornea pachymetry; min.pachy.= minimal pachymetry; ant. elev.= anterior elevation; post. elev.= posterior elevation; y offset value=vertical difference between the vertex normal and the thinnest point of the cornea

Variables	Area under the curve	Std. Error	p value
post.elev. (µm)	0.97	0.017	0.000
ant. elev. (µm)	0.96	0.020	0.000
min.pachy. (µm)	0.90	0.037	0.000
centr.pachy. (µm)	0.88	0.040	0.000
cylinder (D)	0.83	0.042	0.000
aveK (D)	0.82	0.049	0.000
y (mm)	0.79	0.042	0.000

Table 4 shows the sensitivity and specificity identified by cutoff points of posterior corneal elevation.

Table 4. Cutoff point, sensitivity and specificity values of posterior elevation.

posterior elevation cutoff point (µm)	Sensitivity (%)	Specificity (%)
-5.0	100	0
-0.5	100	11.4
1.5	100	27.1
4.5	97.6	50.0
7.5	97.6	67.1
10.5	97.6	80.0
14.5	95.1	90.0
* 15.5	95.1	94.3
17.5	92.7	98.6
19.0	87.8	98.6
21.5	87.8	100
37.5	68	100

* cutoff point

DOI:10.14753/SE.2012.1628

Logistic regression analysis was performed to investigate predictors of two models. The first model was constructed of variables representing classical topographic (average keratometry, cylinder) and central pachymetric findings. Into the second model new variables obtained by the height data of Pentacam (minimal pachymetry, anterior and posterior elevation) were added. The goodness-of-fit of the second model was superior to that of the first (r^2: 0.67 vs. 0.51). For the first model positive predictive value was: 0.75, negative predictive value was: 0.95, for the second model positive predictive value was: 0.92, negative predictive value was: 1.0.

Figure 16 shows the structure of a three-factor model of CFA which showed the best indices of fit (chi-Square p-level: 0.60, RMSEA: 0.001), identifying corneal curvature (CC), corneal thinning (CT) and cone apex elevation (CE) as latent factors responsible for clinical alterations as detected by the measured variables. Good correlation was found between these factors (CC vs. CT: 0.75; CC vs. CE: 0.72; CT vs. CE: 0.75 respectively). The most representative variable for the detection of this corneal shape disorder in the overall model was minimal pachymetry (-0.99), followed by anterior elevation (0.98), keratometry results (0.95), central pachymetry (-0.94), posterior elevation (0.92) and corneal cylinder (0.38). Table 5 demonstrates the results of the confirmatory factor analysis.

DOI:10.14753/SE.2012.1628

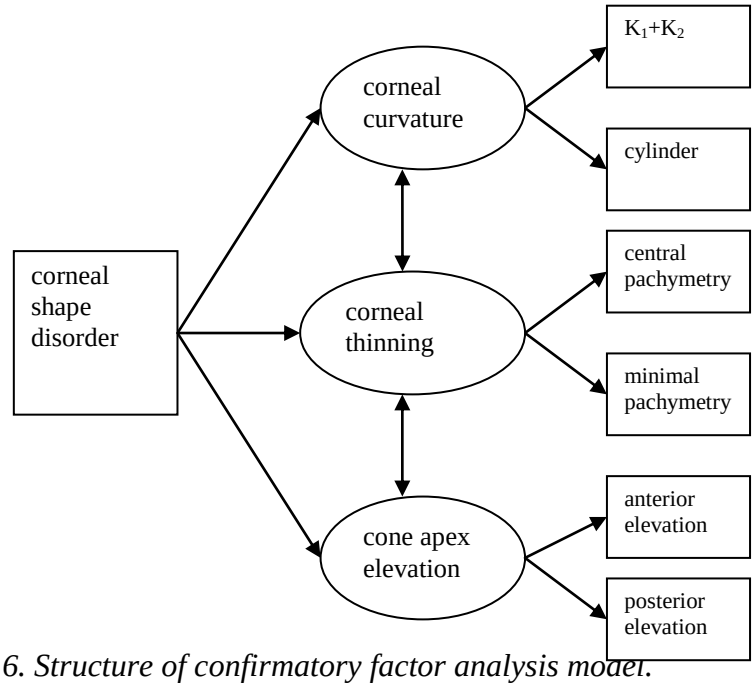

Figure 16. Structure of confirmatory factor analysis model.

Table 5. Results of confirmatory factor analysis (chi-Square p-level: 0.6, Steiger-Lind RMSEA Point Estimate: 0001)

parameter	path coefficient	Standard error
minimal pachymetry (μm)	-0.99	0.000
anterior elevation (μm)	0.98	0.030
K_1+K_2 (D)	0.95	0.153
central pachymetry(μm)	-0.94	0.018
posterior elevation (μm)	0.92	0.036
cylinder (D)	0.39	0.148

DOI:10.14753/SE.2012.1628

4.2. Anterior chamber characteristics of keratoconus (II)

Table 6 shows the mean measurement values in the keratoconus and control groups. Table 7 shows the correlation (r values and P values) between posterior corneal elevation and anterior chamber morphology parameters. The anterior chamber was significantly deeper in the keratoconus group than in the control group at all measurement points (ie, center; 1.0 mm, 2.0 mm, and 3.0 mm paracentral; thinnest). There was no statistically significant difference between the 2 groups in anterior chamber volume, anterior chamber angle, or spherical equivalent. The posterior elevation was significantly higher in the keratoconus group than in the control group and had a strong correlation with minimum pachymetry and central pachymetry. In contrast, no significant correlation was found between the posterior elevation and pachymetry results in the control group. In the keratoconus group, posterior elevation was statistically significantly correlated with ACD in the central cornea ($r = 0.57$), at the thinnest point of the cornea ($r = 0.41$), and 1.0 mm paracentrally ($r = 0.45$). Posterior elevation did not correlate with the ACD 2.0 and 3.0 mm paracentrally, anterior chamber angle, and anterior chamber volume in the keratoconus group (Table 7).

DOI:10.14753/SE.2012.1628

Table 6. Anterior chamber and corneal morphology by group.

	Mean ± SD		T test
Parameter	Keratoconus Group	Control Group	P Value*
Anterior chamber			
Volume (mm^3)	175.28 ± 20.42	160.03 ± 60.82	0.15
Angle (degrees)	37.83 ± 5.49	34.98 ± 7.99	0.06
Anterior chamber depth (mm)			
Central	3.19 ± 0.28	2.83 ± 0.55	<0.001
At minimum pachymetry	3.29 ± 0.33	2.87 ± 0.55	<0.001
1.0 mm paracentral	3.15 ± 0.25	2.82 ± 0.57	<0.01
2.0 mm paracentral	2.83 ± 0.27	2.48 ± 0.71	<0.01
3.0 mm paracentral	2.44 ± 0.29	2.12 ± 0.62	<0.01
Corneal thickness (μm)			
Central	491 ± 43	555 ± 28	<0.001
At minimum pachymetry	469 ± 57	554 ± 26	<0.001
Posterior elevation (μm)	40.77 ± 22.9	−0.63 ± 6.88	<0.001
Spherical equivalent (D)	−3.7 ± 2.7	−2.9 ± 3.7	0.14
Average keratometry (D)	47.90 ± 5.09	43.37 ± 1.33	<0.001

* t test

DOI:10.14753/SE.2012.1628

Table 7.Correlation between posterior corneal elevation and anterior chamber morphology parameters.

	Linear Regression	
Parameter	r	P Value
Anterior chamber		
Volume (mm^3)	0.25	>0.05
Angle (degrees)	−0.10	>0.05
Anterior chamber depth (mm)		
Central	0.57	<0.001
At minimum pachymetry	0.41	0.006
1.0 mm paracentral	0.45	0.02
2.0 mm paracentral	0.27	>0.05
3.0 mm paracentral	0.20	>0.05
Corneal thickness (μm)		
Central	−0.62	<0.001
At minimum pachymetry	−0.75	<0.001
Mean keratometry (D)	0.58	<0.001

On univariable GEE logistic regression analysis, the mean keratometry, posterior elevation, central ACD, ACD at minimum pachymetry, CCT, and minimum corneal thickness were significantly different between normal eyes and keratoconus eyes. However, on multivariable logistic regression analysis, only the ACD at minimum pachymetry remained significant after posterior elevation was entered into the model (Table 8).

DOI:10.14753/SE.2012.1628

Table 8. Results of univariable and the multivariable GEEs to predict keratoconus.

GEE Model/Parameter	OR (95% CI)	QICC	P Value
Univariable			
Posterior elevation	1.44 (1.25-1.65)	29.4	<0.001
ACD			
Central	5.19 (1.9-14.18)	138.16	0.001
At minimum pachymetry	6.03 (2.18-16.67)	135.39	0.001
Pachymetry			
Minimum	0.95 (0.92-0.98)	75.01	0.001
Central	0.95 (0.92-0.98)	90.69	0.001
Average keratometry	1.79 (1.33-2.41)	103.46	<0.001
Multivariable			
Posterior elevation	1.46 (1.25-1.71)	27.74	<0.001
ACD at minimum pachymetry	7.54 (1.35-42.05)	—	0.02

ACD = anterior chamber depth; CI = confidence interval; GEE = generalized estimating equation; OR = odds ratio; QICC = corrected quasi-likelihood under independence model criterion

A piecewise linear regression model to fit linear segments to different ranges of posterior elevation showed a statistically significant explanation coefficient and breakpoint value (Table 9). The linear piecewise model yielded better explanation coefficients and lower AIC values than the linear model, showing the segmented nature of the correlation. Figure 17 shows the regression curves of the 2 models and the estimated breakpoint location determined by the piecewise regression analysis. The curves show that beyond a threshold, the corneal protrusion rate was significantly different. Above 40 μm of posterior elevation, corneal ectasia accelerated by 7 times (regression coefficient ratio) between the second segment and the first segment of the curves (Table 9).

DOI:10.14753/SE.2012.1628

Table 9. Linear and piecewise linear regression results of correlation between posterior elevation and ACD at the minimum pachymetry. CI = confidence interval

Parameter	Mean (95% CI)	P Value
Linear		
Model explanation coefficient (r^2)	0.23	0.001
Akaike information criterion	137.88	—
Piecewise linear		
Regression coefficient		
Of first segment	0.001 (−0.01 to 0.01)	0.85
Of second segment	0.007 (0.003 to 0.012)	0.002
Estimated breakpoint (μm)	40 (36.5 to 43.3)	0.002
Model explanation coefficient	0.41	<0.001
Akaike information criterion	101.67	—

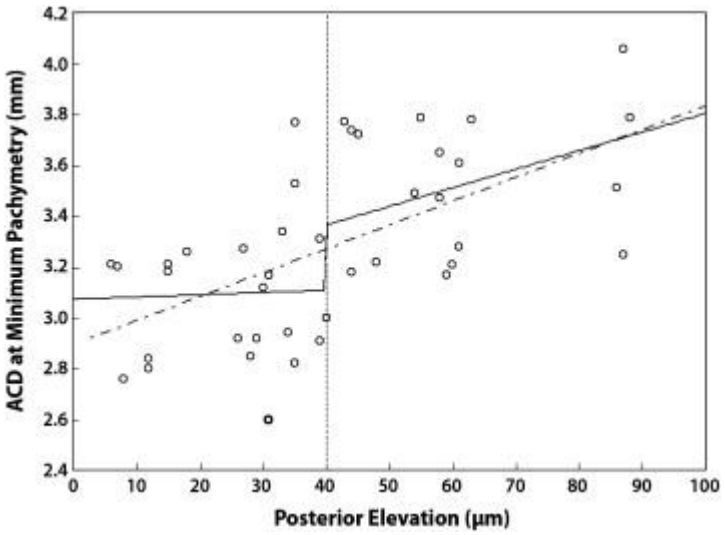

Figure 17. Piecewise linear regression model used to fit linear segments to different ranges of posterior elevation determined a breakpoint of the curve at 40 μm (95% CI, 36.5-43.3 μm, vertical dotted line). This segmented regression model (continuous line) showed better fit to the data than the linear regression model (dotted line) (ACD = anterior chamber depth).

DOI:10.14753/SE.2012.1628

The univariable GEE logistic regression model to validate the threshold value and test the effect of minimum pachymetry had a lowest QICC value of 40.64 and a 450 μm cutoff point for minimum pachymetry. This confirmed that 40 μm was the best cutoff point for posterior elevation.

4.3. Shifting of the line of sight in keratoconus measured by a Hartmann-Shack sensor (III)

Fifty-five eyes of 30 patients with keratoconus and 100 healthy eyes of 50 refractive surgery candidates were included in this study. There were no statistically significant differences between the keratoconus (mean age: 31.5±8.2 years, 13 men, 17 women) and the control groups (mean age: 30.3±10.9 years, 22men, 28 women) in age or sex distribution (p=0.1). There was no statistically significant differences between the refractive state of the eyes in the two group neither, as most of the refractive surgery candidates had a myopic refractive error, mean spherical equivalent in the keratoconic group was: -3.7±2.7 diopters (D), in the control group: -2.86±3.7D, p=0.14.

Internal validation of original data using bootstrapping method showed high consistency with results of the original sample, confirming our selection method statistically applicable.

Table 10 shows the mean and standard deviation values of RMS, HORMS, Zernike polynomials and x,y offset parameters of keratoconic and normal corneas. There was no statistically significant difference between the two groups in total RMS value, which can be explained by the similar refractive states of the two groups. The HORMS values in the keratoconic group were significantly higher than in the control group. The following Zernike terms were significantly higher among keratoconic patients: oblique astigmatism (Z_2^{-2}), trefoil (Z_3^{-3} and Z_3^{3}), vertical coma (Z_3^{-1}), secondary astigmatism (Z_4^{-2} and Z_4^{2}), quadrafoil (Z_4^{4}), pentafoil (Z_5^{-5}), secondary coma and trefoil (Z_5^{-1} and Z_5^{3}). Vertical coma showed the highest values among higher-order Zernike coefficients. There was no statistically significant difference in the x offset values, but y offset showed a marked increase (-0.19±0.38) in keratoconic patients, the negative sign means that the LoS shifted downwards in average.

DOI:10.14753/SE.2012.1628

Table10. Average and standard deviation values of RMS, HORMS, Zernike polynomials and x ,y offset parameters of keratoconic and normal corneas, statistically significant difference ($p<0.05$) marked with *.

	Control mean±SD (μm)	Keratoconus mean±SD (μm)	p
RMS	3.0±1.7	3.06±1.9	0.92
HORMS	0.18±0.14	0.59±0.26	0.000*
Z_2^{-2}	0.052±0.31	-0.397±0.79	0.001*
Z_2^{0}	2.074±2.76	2.594±1.92	0.466
Z_2^{2}	-0.284±0.69	-0.134±0.97	0.430
Z_3^{-3}	-0.048±0.1	0.071±0.25	0.000*
Z_3^{-1}	0.026±0.1	-0.418±0.29	0.000*
Z_3^{1}	0.013±0.06	0.016±0.17	0.534
Z_3^{3}	-0.005±0.06	-0.083±0.19	0.001*
Z_4^{-4}	0.002±0.03	-0.005±0.07	0.368
Z_4^{-2}	0.005±0.04	0.045±0.07	0.000*
Z_4^{0}	0.021±0.05	0.002±0.13	0.868
Z_4^{2}	-0.007±0.04	-0.051±0.11	0.000*
Z_4^{4}	0.011±0.04	0.032±0.05	0.016*
Z_5^{-5}	0.002±0.02	-0.004±0.03	0.033*
Z_5^{-3}	0.009±0.03	-0.004±0.05	0.546
Z_5^{-1}	-0.006±0.02	0.018±0.06	0.045*
Z_5^{1}	-0.002±0.02	-0.005±0.02	0.284
Z_5^{3}	-0.0002±0.02	0.004±0.03	0.014*
Z_5^{5}	-0.005±0.04	-0.001±0.02	0.539
Z_6^{-6}	-0.001±0.02	-0.001±0.01	0.776
Z_6^{-4}	0.001±0.01	0.0001±0.01	0.673
Z_6^{-2}	-0.002±0.01	-0.002±0.01	0.641
Z_6^{0}	0.0055±0.02	0.007±0.03	0.202
Z_6^{2}	0.001±0.01	-0.002±0.03	0.517
Z_6^{4}	-0.001±0.01	-0.002±0.02	0.126
Z_6^{6}	0.0012±0.03	-0.002±0.01	0.845
x offset	0.29±0.38	0.24±0.48	0.22
y offset	0.02±0.33	-0.19±0.38	0.0007*

DOI:10.14753/SE.2012.1628

Our hypothesis was that the LoS shifted in the direction of the cone. To test this, we have calculated the axis of the shift of the line of sight as mentioned above. The cone location can be characterized by the steepest keratometric axis (Ks) on topography, only the topograph always locates this meridian between 0 and 180 degrees, in case of inferiorly located cones we have reversed the Ks to the inferior half of the cornea by adding 180° to the original axis. Figure 18 shows the correlation between the axis of line of sight (LoS) and the axis of the steepest meridian on topography. The correlation was statistically significant (r=0.59, p<0.001).

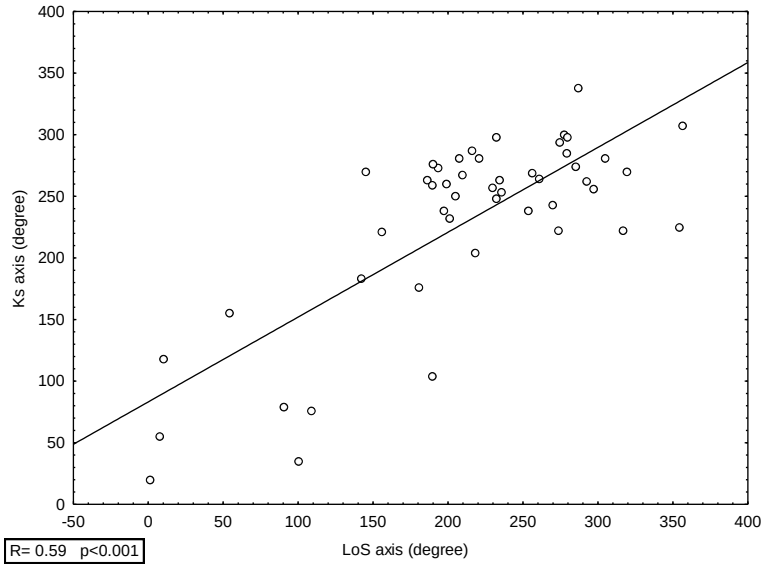

Figure 18. Correlation in keratoconic patients between the axis of the shift of line of sight (LoS) and the axis of the steepest meridian on topography (Ks) which in case of inferior cones is reversed to the inferior half of the cornea by adding 180° to the original axis. The correlation is statistically significant, R and p values were calculated by Spearman rank correlation.

We found a significant correlation between the extent of the shift (hypotenuse) and the negative value of vertical coma (r=-0.39, p=0.004). Figure 19 shows that as vertical coma increases in a negative direction, the line of sight moves farther from the pupil center.

DOI:10.14753/SE.2012.1628

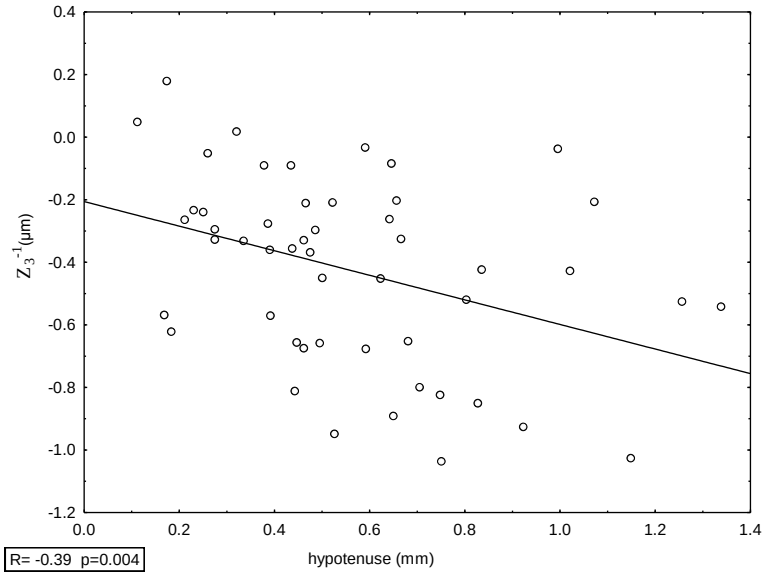

Figure 19. Correlation between the hypotenuse, which is the distance of LoS from the pupil center and vertical coma (Z_3^{-1}) among keratoconic patients. The correlation is statistically significant, R and p values were calculated by Spearman rank correlation.

Figure 20 shows the marked correlation (r=-0.49, p<0.001) we have found between the average keratometry value (aveK) measured by topography and spherical aberration (Z_4^0). According to the diagram, as progression in steepening occurs the spherical aberration (SA) becomes more and more negative, which means that there is an excess of power in the center relative to the pupil margin.

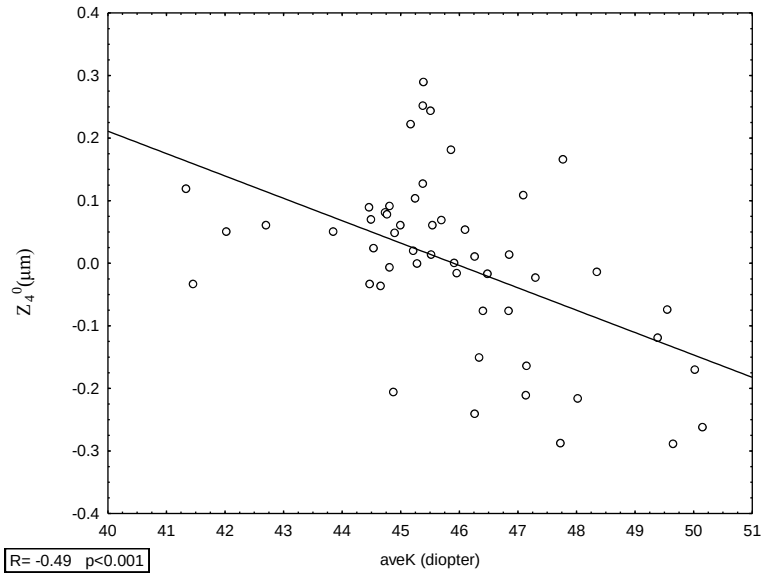

Figure 20. Correlation between the average keratometry value (aveK) measured by topography and spherical aberration (Z_4^0) among keratoconic patients. The correlation is statistically significant, R and p values were calculated by Spearman rank correlation.

DOI:10.14753/SE.2012.1628

We have also found a correlation (r=0.29, p<0.04, Fig. 21) between the size of the hypotenuse, which is the distance of LoS from the pupil center and spherical aberration. As spherical aberration increases, the distance of the LoS from the pupil center increases. We found no significant correlation between average keratometry and the hypotenuse.

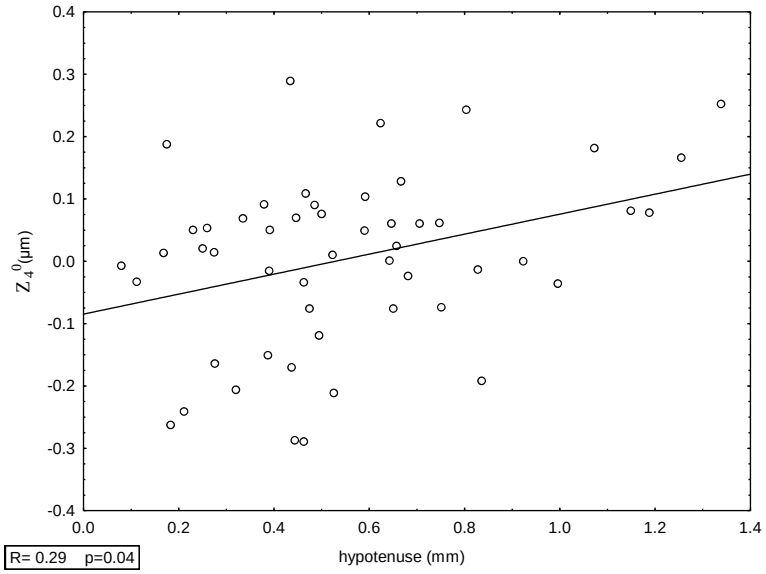

Figure 21. Correlation between the hypotenuse, which is the distance of LoS from the pupil center and spherical aberration (Z_4^0) among keratoconic patients. The correlation is statistically significant, R and p values were calculated by Spearman rank correlation.

Figure 22 represents the axial topography map of a patient with a nasal inferior cone, by whom the LoS is shifted in the same direction and a schematic illustration how the Wasca aberrometer measures the aberrations in a reduced and infero-nasally shifted circular area. In the circle the higher-order aberration map of the same person can be seen. It is evident that the main higher-order aberration is coma and that the line of sight is shifted towards the coma. The aberrometer can measure the aberrations only in a regular circle and its reference axis is always the LoS. This is the explanation why in many cases we couldn't get an aberration map of a larger area than 4-5 mms even if the pupil dilated to 6-7 mms in the dark room.

DOI:10.14753/SE.2012.1628

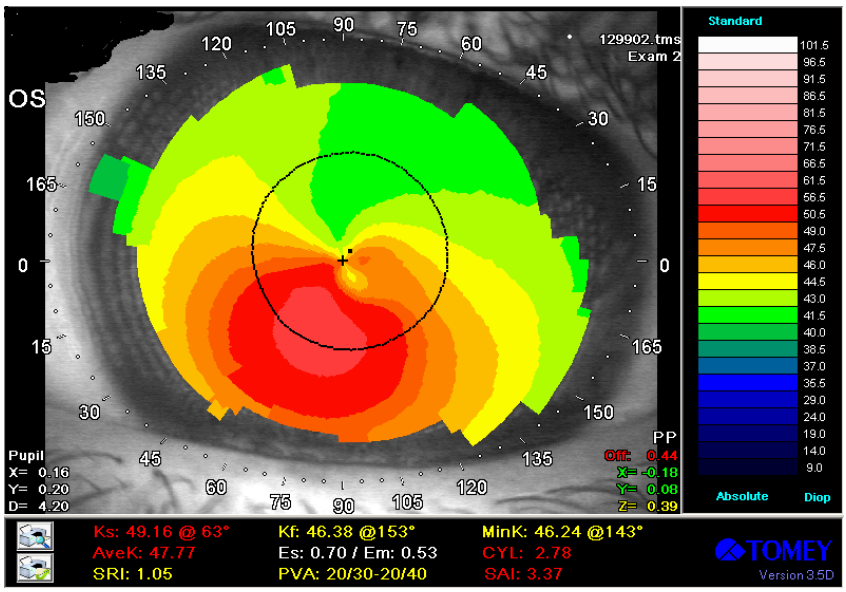

Figure 22A. Axial topography map of a patient with a nasal inferior cone, by whom the LoS is shifted in the same direction.

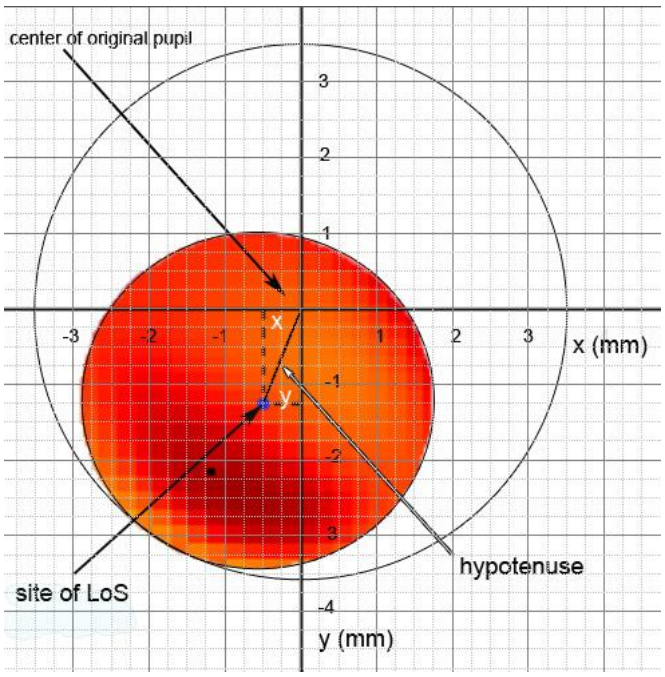

Figure 22B. Schematic illustration how the Wasca aberrometer measures the aberrations in a reduced and infero-nasally shifted circular area in the same patient. y=1.25mm, x=0.46mm, hypotenuse (distance of LoS from pupil center)= 1.33mm.

Finally, a factorial regression model testing the interactive effects of vertical coma and spherical aberration on the shift of LoS had a good fit on our data (r^2=0.69, p<0.001). These result suggests a close correlation between ideally balanced polynomials and the LoS shift.

DOI:10.14753/SE.2012.1628

5. Discussion

5.1. Keratoconus detection with Scheimpflug imaging

5.1.1. Characteristics of elevation based topography

According to the classical, Placido based topographic findings in keratoconus, the most specific changes in the curvature are steepening and protrusion of the cornea usually inferior to the visual axis (2-4,6,42). More recent studies, based on the elevation data obtained by Orbscan and Pentacam measurements indicate, that deformation occurs not only in the anterior, but also in the posterior corneal surface of keratoconus eyes (48,50,53,59,104). As Orbscan derives the posterior elevation map mathematically from the reflection mires of a Placido-disk and 20 slit scans of the anterior segment, there had been caution raised regarding its posterior elevation data measurements (105). Rotating Scheimpflug imaging technology is used by instruments such as the Pentacam (Oculus Inc., Dutenhofen, Germany) to measure the anterior and posterior corneal surfaces, as well as other anterior segment structures. Pentacam uses Scheimpflug imagery and measures 25000 elevation points. This method is independent of axis, orientation and position which is not true for Placido disc based videokeratography. This later method has however significant limitations when trying to describe the cornea with a curvature map. First, there are the physical limitations of a Placido-based, reflecting type system. The area of corneal coverage is limited to about 60% of the corneal surface eliminating important data for many peripheral or para-central pathologies (i.e. pellucid marginal degeneration, keratoconus). Second, there is no information about the posterior surface of the cornea (50,51). Additionally, there are limitations in attempting to reconstruct the corneal surface based on curvature measurements. The standard topographic curvature (axial or sagittal curvature) is a referenced based measurement. It is not a unique property of the cornea. The same shape can have many different ‘curvatures’ depending on which axis is used to make the measurement. The line of sight and the measurement axis of the videokeratoscope are not the same. True topographic imaging implies shape and requires the generation of an X, Y and Z coordinate system. (7,8,41,42,44,45).

Scheimpflug camera displays elevation data not in its raw form (actual elevation data) but compared with some reference shape. The maps typically display how the actual corneal elevation data compares (deviates) with this known shape. The reason for this is to magnify

DOI:10.14753/SE.2012.1628

the differences and allow the clinician a qualitative map that will highlight clinically significant areas. The reason for viewing elevation data in this format is that the actual raw elevation data lacks qualitative patterns that would allow the clinician to easily separate normal from abnormal corneas. Although not an elevation map, the pachymetric map represents the spatial difference between the anterior and posterior corneal surface and in as such is totally dependent on accurate elevation data. In addition to identifying thin corneas, the overall pachymetric distribution may be another indicator of pathology. Normal corneas are typically thinnest in the central region and thicken in the periphery. Displacement of the thinnest region is often seen in keratoconus and may at times predate changes on either the anterior or posterior surfaces (7,8).

Evaluating corneal shape using Scheimpflug imaging may allow validation of the measurements previously obtained by the Orbscan. Ciolino and Belin (9) studied changes in posterior corneal elevation following excimer treatment in 121 myopic eyes using the Pentacam. Although trend lines suggested a relationship between a thinner corneal and more negative posterior corneal surface in LASIK, photorefractive keratectomy (PRK) trend lines are essentially flat. There was no significant difference between the posterior displacement between LASIK and PRK eyes. No LASIK eyes showed significant forward displacement. They concluded that subclinical incidence of post-LASIK ectasia, previously based on Orbscan measurement, may be less than previously thought.

Quisling et al. (59) compared measurements from Orbscan IIz and the Pentacam in eyes with keratoconus. The Orbscan IIz best fit sphere fixed to the apex was compared with the Pentacam posterior best fit sphere with the float option removed. The average best fit sphere radius and average thinnest points were not significantly different between the two systems. The posterior elevation was significantly different, despite similar radii of curvature. This may be due to a difference in data analysis by the two machines. The Orbscan estimates the central 3 mm while the Pentacam images the cornea directly. It was suggested that the Orbscan IIz may be more accurate in the periphery but less so in the center, overestimating the posterior height. Both machines found the location of the cones most commonly located in the inferior temporal quadrant.

Ambrosio et al. (49) used the Pentacam to evaluate normal and keratoconic eyes to determine characteristics which may help to detect keratoconus. The Pentacam yields information regarding the thickness, volume and spatial profile from the three-dimensional model. Corneal thickness at the thinnest point was used to create spatial thickness profiles and volume centered around the thinnest point. Significant differences were found in all positions

DOI:10.14753/SE.2012.1628

of the spatial thickness profile and volume distributions, with lower values for each in keratoconic eyes. Keratoconic eyes were thinner with less volume and a more abrupt increase as one moved outward from the thinnest point of the cornea than normal eyes.

5.1.2. The role of reference body selection in the diagnosis of keratoconus

The corneal surface is variably aspheric and toric, this diversity is even more pronounced in keratoconic patients. Approximating posterior corneal surface to a conic is useful as it permits the description of its shape by the apical radius and the rapidity of steepening or flattening from the apex. The ellipso-toric model besides corneal asphericity incorporates the difference in curvature between the two principal meridians (48, 106). Therefore an aspherical and toric reference surface like a toric ellipsoid would lie closer to the actual corneal surface and enhances local changes more sensitively than a reference sphere. There are several previous papers concerning the discriminating potential of posterior elevation in keratoconus, however there is no accordance in reference body selection, which makes the comparison of different study result difficult. The selection of reference body influences the magnitude of posterior elevation and thus the identified cutoff values for discriminating keratoconic corneas from normal.

There are several previous papers reporting posterior elevation cutoff values characteristic of keratoconus, however there is no accordance in reference body selection, which makes the comparison difficult. The disparity between the different results obtained by Pentacam and Orbscan can be explained by the different scanning methods, but also by the reference body selection. A larger diameter best fit sphere results in larger posterior elevation values (48,53,59,104).

Toric ellipsoid reference bodies approximate the aspheric corneal surface seen in keratoconus better than spherical models. This concept can be better understood when looking at the schematic illustration of posterior elevation calculating method on Figure 23. An increased prolateness results in higher elevation values in the center. It is also apparent that when a toric ellipsoid reference surface is used the central vaulting above the reference surface has less variation and posterior elevation values around the cone apex are smaller than with a BFS. The selection of reference body also determines the sign of elevation data in corneal astigmatism. With toric ellipsoid as a reference body, surface elevation data along the steep meridian at the mid-periphery are positive, while data along the flat meridian are negative. Using sphere as a reference surface corneal astigmatism shows negative elevation

DOI:10.14753/SE.2012.1628

data along the steep meridians and positive elevation data along the flat meridians. It can be also observed that the toric ellipsoid reference body crosses the cornea twice at the steepest meridian, while only once at the flat meridian. This is probably due to the variable asphericity values in different meridians of the cornea. Even in healthy corneas the value of asphericity changes between meridians, the most oblate meridian was found to be horizontally (100,101,105,106).

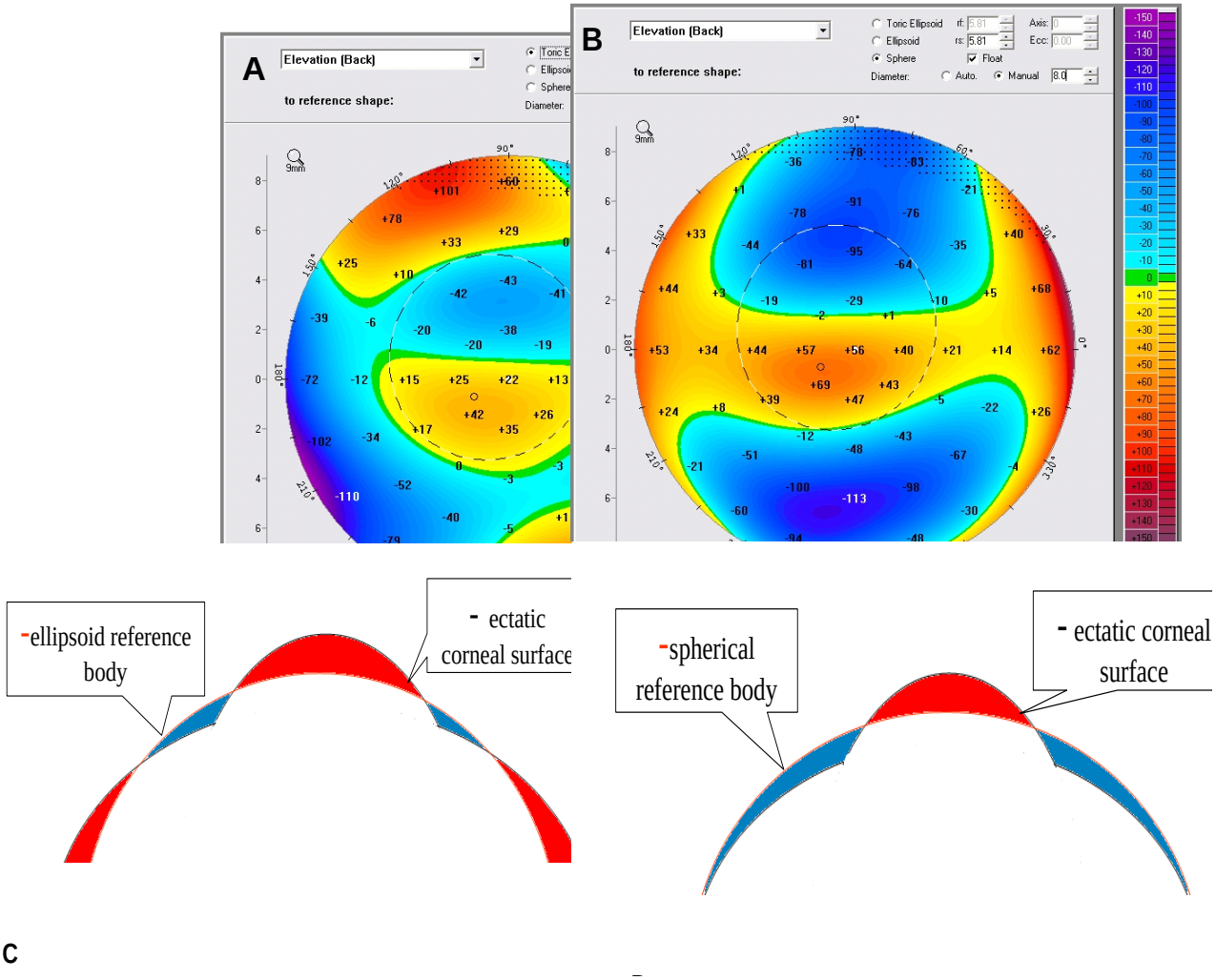

Figure 23. Posterior elevation maps of a keratoconic patient with a best fit toric ellipsoid (BFTE) reference body (A) and a fixed 8mm best fit sphere (BFS) reference body (B). Schematic cross-sectional view of the cornea and ellipsoid reference body (C) and spherical reference body (D) in the steepest meridian (99°). Areas colored red correspond to corneal elevation relative to reference surface, elevation: + value. Areas colored blue correspond to corneal depression relative to reference surface, elevation: - value. Site of the thinnest point marked: ◦. (images are from our own database, schematic illustrations are drawn by the author)

DOI:10.14753/SE.2012.1628

By definition, an astigmatic surface is one that has two meridians of different curvature. When these principal meridians are orthogonal (90° apart) the surface is said to be regular. Regular astigmatism shows a classic pattern where the flat meridian is raised off the BFS and the steep meridian is below (or depressed) the BFS (Fig. 25). The larger the astigmatism the greater the difference between corresponding points on the principal meridians. Additionally, the further you go out from the centre the greater the deviation from the BFS. Irregular astigmatism is by definition where the principal meridians are non-orthogonal. This is readily apparent in the standard elevation subtraction map. Mild changes may still be associated with good best spectacle corrected vision (BSCVA), but larger amounts of irregular astigmatism are typically associated with a reduction in BSCVA. Although the BFS is still best for screening, a toric ellipsoid can mimic what is correctable by spectacles (both sphere and cylinder) and differences from the toric ellipsoid should correlate to the reduction in BSCVA (this is effectively what some have called an irregularity map). Irregularly irregular corneas are so distorted that the principal meridians can often not be identified. These corneas are almost always pathologic, associated with a significant reduction in BSCVA and may be seen in conditions such as keratoconus, anterior dystrophies and corneal scarring. An ectasia is a protrusion of the corneal surface. These can occur on the anterior corneal surface, the posterior surface or both. In keratoconus, when a BFS is fit to a cone the apex of the cone appears as a circular area of positive deviation off the BFS (‘island’). This pattern (‘island’) is distinct from the positive elevations seen on the flat meridian of an astigmatic eye. The purpose of utilizing the reference surface is to allow for qualitative separation of normal and abnormal corneas. The magnitude (height) of the island corresponds to the degree of elevation off the more normal cornea. The size of the base of the island corresponds to the extent of the cornea involved in the ecstatic process. The location of the ‘island’ more clearly demonstrates the location of the cone. (48,53,59,104,106).

DOI:10.14753/SE.2012.1628

5.1.3. The use of elevation data in the diagnosis of keratoconus (I)

In our first study ROC curve analysis showed, that posterior elevation was the most effective parameter in the diagnosis of keratoconus. A cutoff value of 15.5μm had 95.1% sensitivity and 94.3% specificity for discriminating normal eyes from keratoconus. De Sanctis et al (104) also found posterior elevation a sensitive parameter for the detection of keratoconus with Pentacam, they identified a cutoff value of 35 μm for keratoconus and 32 μm for subclinical keratoconus. Rao et al (106) has found a posterior elevation greater than 40 μm as a diagnostic index for keratoconus using Orbscan data. Fam et al (48) identified a cutoff value of 16.5 μm for the anterior elevation as the most sensitive index with ROC curve analysis for discriminating keratoconus with Orbscan. They have found that posterior elevation of ≥ 40 microns had a sensitivity of 57.7% and specificity of 89.8% when keratoconus and keratoconus suspects were classified from normals from the study. The sensitivity and specificity of posterior elevation increased to 99% and 92.8%, respectively, when keratoconus was differentiated from normals. They find that the posterior elevation was limited in its clinical application compared to anterior elevation and anterior elevation ratio. They have concluded that anterior corneal elevation is a better indicator than posterior elevation of keratoconus and suspected keratoconus. The disparity between the different results obtained by Pentacam and Orbscan can be explained by the different scanning methods. The Orbscan II is a hybrid system that acquires data through slit-scanning (projective) and Placido ring (reflective) technology. Slit-scan and corneal pachymetry data are used to generate relative elevation maps of the anterior and posterior cornea. Placido disk reflections supplement slit-scan data to generate curvature-based maps, such as axial and meridional (tangential) keratometric maps. An elevation map is calculated by fitting the corneal shape to a best-fit sphere (BFS). Without a BFS, minute variations in corneal elevation may be masked by the overwhelmingly large corneal curvature. Micro variations in corneal elevation (μm) may be optically significant but can be lost in the overall sagittal depth of the cornea (mm). Elevations are plotted against a sphere for which the algebraic sums of elevations and depressions are equal.

The cutoff point of 38μm, identified by de Sanctis et al, using our data, has a sensitivity of 68% and a specificity of 100%. Both studies have used the same settings for posterior elevation, the maximum values above the BFS in the central 5 mm of the cornea, using the float option. The explanation for the diverse results is most probably the obvious heterogeneity of disease severity among previously diagnosed patients. Moreover, our study included already known keratoconus patients, from mild to moderate disease severity, severe

cases were excluded. De Sanctis et al have subdivided their patients in two groups, subclinical keratoconus and keratoconus groups. Further investigations on larger population is required to determine precise cutoff values for posterior elevation.

In contrast to ROC curve analysis, confirmatory factor analysis (CFA) is not used for discriminating keratoconus from normal corneas, but it tries to identify and rank the underlying mechanisms leading to the corneal shape disorder observed in the disease. Therefore this analysis was performed only on the keratoconic patient group. CFA is a statistical tool, which avoids the use of any pre-established gold standard diagnostic method (103). During CFA the most representative variables can be determined using correlation matrices and several model structures can be examined. To our knowledge, this is the first application of CFA in the evaluation of keratoconus. In the CFA model, we examined three topographic parameters [(flat and steep keratometry, cylinder) characterizing corneal curvature factor], two pachymetric parameters [(minimal and central pachymetry) the corneal thinning factor] and two elevation parameters [(anterior and posterior elevation at the apex of the cone) cone apex elevation]. All these parameters have been shown to affect corneal morphological alteration observed in keratoconus. The size of the path coefficients (Table 5) show the ability of the parameter to quantify the corneal damage. A path coefficient of 1 corresponds to a measurement that perfectly quantifies the disease. In our model best results were obtained for the minimal pachymetry (-0.99), followed by anterior elevation (0.98), keratometry results (0.95), central pachymetry (-0.94), posterior elevation (0.92) and corneal cylinder (0.38). These results show, that elevation measurements and localization of the apex of the cone by corneal pachymetric map play an important role in the detection of disease progression. Before the advent of Orbscan and Pentacam, these data could not be measured. The same hypothesis is supported by the results of the logistic regression analysis, according to which the model completed with the height data of the Pentacam shows a better ability for disease prediction.

Although it has been suggested that an increase in posterior elevation may be the earliest sign of subclinical keratoconus (104) indices derived from Placido-disk based videokeratography may be also sensitive in discriminating this condition, which is in large part defined on the basis of topographic patterns produced with this method. However, in eyes with subclinical keratoconus, the Pentacam rotating Scheimpflug camera may add useful information to Placido disk-based videokeratography. Axial curvature analysis, provided by the latter method, suffers from some limitations when studying an abnormal shape. Axial curvature analysis is based on the assumption that the reference axis used to generate the

DOI:10.14753/SE.2012.1628

maps is the same as the visual axis and the corneal apex. In many normal eyes, the corneal apex and the corneal sighting point do not correspond, and Placido-disk based videokeratography may generate incomplete or sometimes misleading pictures (42,50,51). Because the cornea is analyzed around a point other than its center, a normal aspherical surface may generate an asymmetrical bow-tie pattern or inferior steepening, which are the commonest patterns seen in subclinical keratoconus. In such eyes, the Pentacam rotating Scheimpflug camera may help to distinguish normal from abnormal corneal shapes, because this system directly acquires elevation points from the corneal surfaces.

5.1.4. Comparative analysis of anterior chamber characteristics of keratoconus (II)

The result of the second study—that the anterior chamber was significantly deeper in eyes with keratoconus than in normal eyes—confirms previous studies using Scheimpflug imaging. The Pentacam system can evaluate the cornea and anterior segment of the eye from the anterior surface of the cornea to the posterior surface of the lens. Anterior chamber depth is a major parameter of the Pentacam. In the study of Emre et al. (53), the mean ACD in all keratoconic eyes was higher than in the control group. Even in mild cases, the ACD was significantly deeper than in the control group and the ACD became deeper as the disease progressed. In their study, the difference in mean ACD between the severe and mild keratoconic groups was 0.46 mm, an almost 14% increase in depth with the progression of the disease. This increase in ACD was larger than the change in thinnest corneal thickness (TCT). They have found that the anterior protrusion of the central corneal may be a source of the increase. Accurate measurement of the ACD is of paramount importance in the implantation of phakic intraocular lenses (pIOL) may be implanted for the management of keratoconus. Thus, the progressive increase in ACD may be an advantage in keratoconic patients in terms of implantation of pIOLs.

More recent studies based on the elevation data obtained by slit-scanning topography and Scheimpflug measurements indicate that deformation occurs in both the anterior surface and the posterior corneal surface in eyes with keratoconus (50, 104,107). Rotating Scheimpflug imaging not only measures the thickness of the cornea over a wide area but also finds the exact location of the minimum pachymetry and the maximum elevation points, allowing assessment of morphologic parameters across the anterior chamber. In a study by

Meinhardt et al. (107), ACD measurements by Scheimpflug imaging showed less intraobserver variation than measurements by partial coherence interferometry, whereas Buehl et al. (108) found that both are reliable, easy-to-use methods for measuring pachymetry and ACD.

In our study, we characterized the severity of keratoconus using the posterior corneal elevation because it has been described as the most sensitive indicator of keratoconus (50,104). Results in our linear piecewise regression analysis suggest there is a specific threshold level of disease progression at which level the rate of protrusion is significantly elevated. Linear piecewise model had better fit to data than linear regression analysis, confirming the different correlation across the data set. The jump of the regression line at the threshold level supports the separated nature of keratoconus cases below and above this threshold level. The higher regression coefficient of the second segment of piecewise regression curve indicates a closer correlation between corneal protrusion and anterior chamber deepening, suggesting that decreased corneal stiffness is a more important determinant of corneal ectasia in advanced forms.

Ciolino et al. (9) used Pentacam imaging after laser in situ keratomileusis in healthy eyes over a 14-month follow-up. They found no progressive changes in the posterior corneal surface that would be typical of ectasia. In addition, the posterior corneal elevation was not correlated with the residual stromal bed (RSB) thickness in these healthy eyes, suggesting that corneal thinning does not cause corneal ectasia when a minimum RSB of 327 μm is respected. In contrast, our results in corneas with keratoconus proved that progressive forward displacement of the posterior corneal surface correlates with corneal thinning and anterior chamber deepening. The segmented nature of the correlation between corneal parameters and ACD suggests that beyond a certain threshold, ectatic corneas have decreased resistance to intraocular pressure. After our keratoconus cases were dichotomized according to the 40 μm cutoff value, a univariable GEE model with minimum pachymetry as the predictor identified 450 μm as the cutoff point of minimum pachymetry for the best prediction results and a validated posterior elevation cutoff value. We identified the threshold value for central pachymetry as well because it can be measured during later examinations using commercially available instruments.

Hysteresis, a parameter that characterizes the biomechanical status of the cornea, is lower in eyes with keratoconus than in normal eyes (109). There is decreased stiffness and increased extensibility of keratoconus tissue relative to normal tissue; this could be a consequence of abnormal collagen lamella in the areas of ectasia (90). Collagen crosslinking (CXL) is a recently introduced therapeutic method that effectively stabilizes the cornea in

eyes with keratoconus by increasing corneal rigidity (110). Because CXL requires a minimum stromal bed of 400 μm and, according to our results, disease progression is more rapid beyond a threshold level, we recommend treatment be performed before this breakpoint. Finally, posterior elevation and minimum pachymetry results seem to be useful parameters in following corneal protrusion in eyes with keratoconus. Moreover, the threshold levels we identified will further increase the precision of assessing progression of the disease.

5.2. Keratoconus detection with aberrometry (III)

Irregular corneal astigmatism is the hallmark of keratoconus. Irregular astigmatism and higher order aberrations cannot be assessed using clinical refraction. Instead, Placido disk-based videokeratography to evaluate curvature and elevation is better able to define irregular astigmatism. Corneal topography using videokeratography is currently the most commonly used diagnostic modality for diagnosing keratoconus when obvious clinical signs of the disease are absent. The diagnosis of keratoconus can be challenging. Early to moderate cases may not present with typical microscopic signs such as stress lines or obvious protrusion of the cornea. Missed diagnosis occasionally can lead to a disastrous outcome, for example, when refractive surgery is performed on a cornea at risk. Earlier diagnosis of keratoconus would allow identification of the intervention modality that is best suited for a patient. In subtle cases, this may allow clinicians to provide earlier intervention and a more accurate clinical prognosis. Earlier diagnosis could have a great impact on clinical decision-making with respect to refractive surgery. The development of better wavefront criteria for keratoconus and suspected keratoconus has the potential for widespread clinical applications, allowing improved health care delivery through imaging that is fast, relatively inexpensive, and noninvasive (62-65).

More recently, wavefront analysis has been introduced in the field of refractive surgery. Wavefront analysis is able to measure higher order aberrations and irregular astigmatism beyond simple sphere and cylinder. The optical aberrations of the eye are assessed using aberrometers such as the Hartmann-Schack aberrometer. Higher order aberrations are represented in mathematical calculations such as point spread function and Zernike polynomials. For practical reasons, ophthalmology only deals with approximately the first 10 levels of higher order aberrations. The wavefront method is reported to discern refraction of the eye to within 0.05 D, with approximately 25 to 50 times greater accuracy

DOI:10.14753/SE.2012.1628

than phorometry, autorefraction, or topographic analysis. Furthermore, because it analyzes different data points compared to topography, wavefront has the potential to become another sensitive and specific diagnostic tool in keratoconus (65-67).

Currently, a variety of aberrometers, providing measurements of lower order aberrations as well as higher order aberrations, have been widely used to measure monochromatic aberrations of the human eye in pre- and postoperative examinations for refractive surgery.1-3 One of these instruments, the Wavefront Supported Custom Ablation (WASCA) aberrometer (Carl Zeiss Meditec AG, Jena, Germany), which works in accordance with the Hartmann-Shack principle. A Hartmann-Shack device uses a narrow laser beam that is sent along the ocular line of sight into the eye, where it reflects on the retina. This reflection serves as secondary source that illuminates the pupil area from behind. The outgoing light is then guided through a set of relay lenses that projects the pupil plane onto an array of tiny lenses that splits up the wavefront into a number of individually focused spots on a charged coupled device camera. Because of focal shift, the resulting spot pattern shows spot displacements compared with the reference positions. This way, the wavefront slopes are determined for the entire pupil at once (114,116,117).

In our study eyes with keratoconus had significantly more higher-order aberrations than normal control individuals, while there was no statistically significant difference in whole eye RMS values, which is probably due to the fact that myopia and astigmatism was a common refractive error among refractive surgery candidates. It has been described in several papers previously that the dominant aberration of keratoconic patients is vertical coma (62 - 67,111-115). According to our findings, vertical coma was the dominant higher order aberration in keratoconus and there were significant differences in higher order astigmatic polynomials, trefoil and secondary coma also. These aberrations can be attributed to the characteristic cone shape and the inferior shift of the cone's apex (64, 66).

5.2.1. Optical and visual axes of the eye

The eye is a decentered optical system with non-rotationally symmetric components. The principle elements of the eye's optical system are the cornea, pupil, and the crystalline lens. Each is decentered and tilted with respect to other components rendering an optical system that is typically dominated by coma at the foveola. The eye is also an imaging device designed to form an in-focus inverted image on a screen. In the case of the eye, the imaging screen is the retina. However, unlike film, the "grain" of the retina is not uniform over its

DOI:10.14753/SE.2012.1628

extent. Instead, the grain is finest at the foveola and falls off quickly as the distance from the foveola increases. Consequently, when viewing fine detail, we rotate our eye such that the object of regard falls on the foveola. Thus, with respect to an individual's ability to see fine detail, aberration at the foveola has the greatest impact.

There are two axes of interest which are centered on the foveola—the visual axis and the line of sight. In object space, the visual axis is typically defined as the line connecting the fixation object point to the eye's first nodal point. In contrast, the line of sight is defined as the (broken) line passing through the center of the eye's entrance and exit pupils connecting the object of regard to the foveola (Figure 24). The line of sight is equivalent to the foveal chief ray. The visual axis and the line of sight are not the same and in some eyes the difference can have a large impact on retinal image quality (98,116,117).

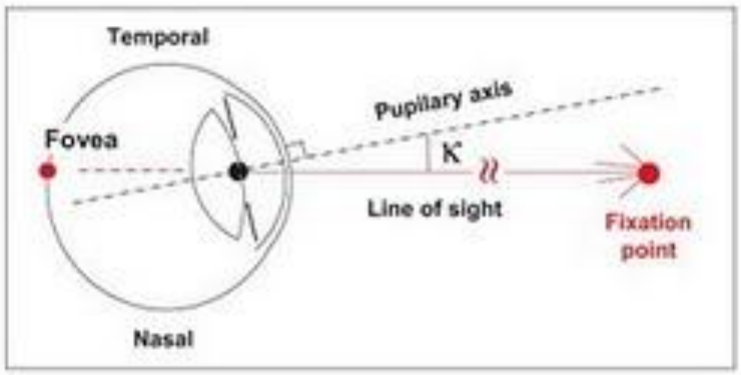

Figure 24. Image illustrates the position of the pupilary axis and the line of sight (122).

The optical industry has a tradition of calculating the optical aberration of systems with respect to the center of the system's exit pupil. In a centered optical system using the center of the exit pupil as a reference for measurement of on axis aberration is the same as measuring the optical aberration with respect to the chief ray from an axial object point.

It is the committee's recommendation that the ophthalmic community remain in optical industry tradition and use the line of sight as the reference axis for the purposes of calculating and measuring the ocular optical aberrations. The rationale is that the line-of-sight is the chief ray for the fixation point and therefore aberrations measured with respect to this axis will have the pupil center as the origin of a Cartesian reference frame (117).

DOI:10.14753/SE.2012.1628

The angle between the pupillary axis and the line of sight is the angle lambda. Our primary observation was, that keratoconic patients had a greater angle lambda, than control patients and the difference was more pronounced in the vertical direction than in the horizontal. To evaluate the nature of this shift and find possible explanations for the direction and magnitude of the displacement we performed vector analysis of the LoS displacement and astigmatic axes.

Our hypothesis, that the shift in the LoS is an internal compensation mechanism to reduce corneal coma caused by keratoconus was confirmed by result of vector analysis as the axis of the shift of the LoS showed a marked correlation with the steepest keratometric axis on topography. Since the steepest keratometric axis characterizes the location of the cone1 the axis of shift of LoS corresponds to the location of maximal protrusion. In addition a correlation was found between the hypotenuse, which is the distance of LoS from the pupil center and the increase of vertical coma in the negative direction. The negative sign of vertical coma means that there is a relative phase retardation of the wavefront in the inferior cornea due to the longer intraocular light path caused by inferior corneal protrusion (65). The displacement of the LoS also occurred inferiorly in most of cases (Figure 18).

5.2.2. Spherical aberration in keratoconus

We have also found evident correlation between the distance of the LoS from the pupil center and the spherical aberration (Figure 21). Spherical aberration is a rotationally symmetric aberration in which the light rays that pass through the paraxial zone of the pupil focus at a different distance than the rays that pass through the marginal pupil (118).

In a normal eye a certain quantity of positive spherical aberration is present, which is considered physiological and is compensated for, at least in part, by the internal optics (121,122).

Following myopic photoablative treatment, the effect of reduction in the spherical aberration due to flattening is generally not sufficient to compensate for the increase in spherical aberration due to the substantial variation in shape obtained with the majority of the current ablation profiles. This effect is even greater in the incisional operations of radial keratotomy, where with equal dioptric correction, the cornea becomes even more oblate. The opposite occurs with hyperopic treatments, as the current ablation profiles produce a hyper-prolate cornea. This variation in shape produces a negative spherical aberration, which usually is not compensated by the increase in positive from the increased curvature (101,117).

DOI:10.14753/SE.2012.1628

The spherical aberration of the anterior corneal surface is added to that of the posterior surface and crystalline lens. These will tend to counterbalance if they are of opposite signs. If all of the components of spherical aberrations do not mutually compensate, the image of a point-object will consist of a disk surrounded by a diffused halo. If the overall spherical aberration is not excessive, a slight loss in contrast transfer will be present, with an improvement in the depth of the field. The latter phenomenon is due to the multifocal effect of the spherical aberration. This is the reason why, in the event of residual ametropia, eyes operated by corneal refractive surgery have a better unaided visual acuity than would be expected on the basis of the residual refractive error. A slight residue of spherical aberration may also prove useful in the event of presbyopia. This is the principle of some types of multifocal contact lenses with simultaneous vision or multifocal intraocular lenses, which have been created in such a way as to produce a certain degree of spherical aberration. With these lenses, if the spherical aberration is positive (as in a myopic treatment), the center of the pupil is used for distance vision and the peripheral zones for near. If the spherical aberration is negative (as in a hyperopic photoablative treatment), the center is for near vision and the periphery for distance (118).

By convention, spherical aberration is positive, when the marginal rays focus ahead of the paraxial rays, whereas it is negative when the opposite is true. The magnitude of spherical aberration depends on entrance pupil diameter, radius of curvature, refractive index and the value of asphericity. Positive spherical aberration is greater the more the cornea is oblate and it becomes negative if the surface is more prolate. As progression in keratoconus occurs, the cone bulges anteriorly, the cornea thins and steepens, the cornea becomes more prolate, which explains why the spherical aberration becomes more negative as the average keratometry value increases. We have also found a correlation between the size of the hypotenuse and SA. With an increasing spherical aberration, the LoS became more decentered. If the apex is not centered on the visual axis a prismatic effect, astigmatism from oblique incidence and coma occurs (119). Kollbaum et al. demonstrated that as spherical aberration is decentered, coma is induced (120). They also stated that depending on the sign of the eye’s inherent coma, typical decentration of a spherical aberration-correcting lens could eliminate or change the direction and/or magnitude of the coma. These findings suggest that the decentration of the line of sight is an internal compensation mechanism of the eye in order to find the ideal balance between spherical aberration and coma. This hypothesis was confirmed using factorial regression in our study which proved the interactive nature of these polynomials on the shift of LoS.

DOI:10.14753/SE.2012.1628

Previous investigations have revealed that there is a balance between corneal aberrations and the aberrations of the internal optics of the eye that results in smaller ocular aberrations (121,122). Kelly et al have found a correlation between angle kappa and corneal lateral coma. They stated that shifting the location and alignment of the optical elements of the eye may be a mechanism how corneal coma is compensated (121).

5.2.3. The pupil apodizing and Stiles-Crawford effect

Figure 24B shows a schematic illustration how the Wasca aberrometer measures the aberrations in a reduced area in a keratoconic patient. The pupil apodizing effect of the Stiles-Crawford effect (SCE) has a similar impact on image formation. This effect means that light entering on or near the receptor axis will have an increased effect on photoreceptors, and the sensitivity for light entering the pupil 4 mm from the peak of the SCE is about 16% of the peak sensitivity (123). It is due to the SCE that the marginal rays from the relatively decentered pupil edge have a diminished visual impact on image formation of keratoconic patients.

Geometrical optics gives a serviceable description of the role of the eye's pupil in admitting the rays that contribute light to the image formed on the retina (Figure 25). To a first approximation, the rays passing through the centre of the pupil strike the retina head-on. The rays coming in near the edge of a fully dilated pupil (approx. 8 mm in diameter) will have an obliquity of approximately 10°. In visual experiments, although the object and its resultant retinal image remain fixed, the location and size in the pupillary plane of the rays can be controlled either by placing an artificial aperture in front of the eye or by a special mode of imagery, called Maxwellian viewing, in which auxiliary optical components in the light beam limit the pupillary region through which it passes into the eye. In either case, the data to be discussed are based on the effect of the pupil entry point on the way light affects the visual process (124).

DOI:10.14753/SE.2012.1628

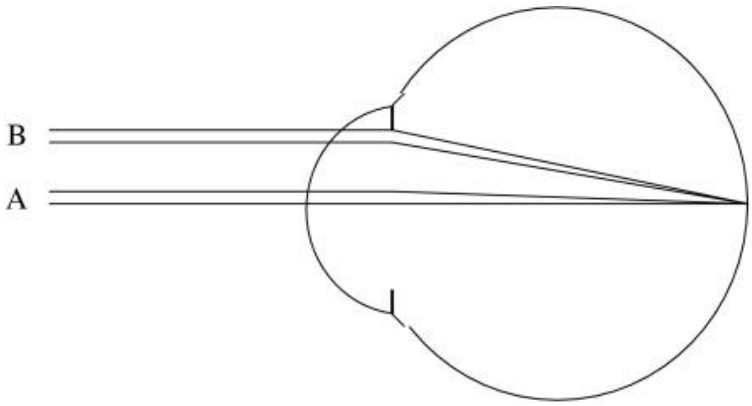

Figure 25. Schematic eye with a wide pupil showing two identical bundles of rays from a distant object focused on the retina that enter through different pupillary regions: A, the centre, and B, near the edge (124).

It is now unanimously accepted that the Stiles–Crawford effect has its origin somewhere in the retinal receptor cells and the photon capture by the photopigment molecules. Because these cells' diameter approaches that of the wavelength of light, it is important to know the spectral dependency of the Stiles–Crawford effect. When we try to find an explanation of the Stiles–Crawford effect, attention centers on the retinal receptor cells and, particularly on rod–cone differences. A variety of morphological factors bears on the approach to an explanation of directional sensitivity. The overall shape of cones varies depending on their retinal location, the ones in the centre of the fovea having thin, long outer segments resembling rods. Histological examinations have revealed that cone's outer segments are tapered though the taper in the foveal centre is very slight. Cones differ from rods at the levels of the cell nucleus, the inner segment and the joining portion, called the ellipsoid; however, in all these dimensions, cone measurements vary markedly between the fovea and the retinal periphery, where the cells are several times wider and prominently tapered. The phototransduction process takes place in the outer segments. Cone photopigments are located in folds of the cell membrane and the rod pigment rhodopsin in stacks of intracellular discs. These polar molecules have a forward-pointing directional acceptance lobe, which at the maximum would follow a cosine law, cosine squared if the calculation is in terms of the intensity of the radiation. For light entering near the edge of a very wide pupil (say, 8 mm in diameter) when the obliquity angle is 10° or less, this would reduce acceptance by only a few per cent and is quite insufficient to account for the actual attenuation of obliquely incident light in cone vision. (123,124).

Our study however has a few limitations. We could not include advanced keratoconus patients in the keratoconus group due to the difficulty of digitalizing the image using the

DOI:10.14753/SE.2012.1628

Hartmann-Shack sensor, so we don't know how the site of the line of sight changes in these patients. The other limitation is that there is an ambiguity in locating the pupil center, since its location depends on the pupil diameter. As mentioned by Kollbaum et al (120) the eye is a dynamical biological system, which accommodates, the tear film, the eye, the pupil, the lens moves continuously. This causes a variability in the detection of aberrations and the localization of the LoS. The visual aberrations in keratoconus also depend on the cone shape, dimension, location and its distance from the visual axis (125). Our study did not take into consideration these parameters. Involving these factors could probably be helpful to better understand the underlying mechanisms responsible for the shifting of line of sight observed in keratoconus.

6. Conclusion

According to the classical, Placido based topographic findings in keratoconus, the most specific changes in the curvature are steepening and protrusion of the cornea usually inferior to the visual axis. Pentacam rotating Scheimpflug camera adds useful information to Placido disk-based videokeratography. According to the elevation data obtained by Pentacam, deformation occurs not only in the anterior, but also in the posterior corneal surface of keratoconus eyes. An increase in posterior elevation may be the earliest sign of keratoconus.

We have demonstrated in our first study (I) among the firsts in the international literature the diagnostic capability of the different parameters obtained by the Pentacam. ROC curve analysis showed, that posterior elevation was the most effective parameter in the diagnosis of keratoconus. A cutoff value of 15.5μm had 95.1% sensitivity and 94.3% specificity for discriminating normal eyes from keratoconus. We have found an optimal cutoff point for posterior elevation, which was 15.5 μm for the discrimination of keratoconus corneas from normals. Logistic regression analysis showed best fit to the data for the model completed with the height data of the Pentacam. Confirmatory factor analysis (CFA) explained a three factor model satisfactorily showing minimal pachymetry (-0.99), anterior elevation (0.98) and keratometry (0.95) as the most representative clinical variables of the disease. Central and minimal pachymetric and keratometric parameters measured by the Pentacam camera can also effectively discriminate keratoconus from normal corneas serving as a useful diagnostic tool for disease staging. We were the first authors in the international literature, who used a CFA to determine the differentiating ability of keratometric and

DOI:10.14753/SE.2012.1628

elevation parameters of keratoconus. Our findings provide a useful tool for the detection of the disease. The posterior elevation cutoff value, which we have identified can serve as a diagnostic guide in the screening of refractive surgery candidates.

In our second study (II) we have demonstrated first in the international literature, that there is a threshold level of posterior corneal elevation and corneal thickness values beyond which the level of corneal protrusion in keratoconus is accelerated According to our results anterior chamber depth (ACD) in keratoconus significantly correlated with posterior elevation. In the multivariable GEE model, posterior elevation and ACD at minimum pachymetry were significant predictors of keratoconus. Segmented analysis of the correlation between posterior elevation and central ACD showed a better fit to data than linear regression and identified a 40 μm threshold level for posterior elevation. The GEE determined 450 μm as a similar threshold for central corneal thickness. This finding may serve as a helpful indication for the timing of surgical intervention or riboflavin treatment of the disease.

Understanding the characteristics of ocular higher order aberrations owing to keratoconus might be very useful to differentiate early cases from simple myopia or myopic astigmatism. In our third study (III) we evaluated ocular wavefront aberrations owing to keratoconus compared with normal controls. We have described first in the international literature the changes in the axis of line of sight (LoS) among keratoconic patients. Higher order root mean square error, primary and secondary vertical coma, trefoil, secondary astigmatism and y offset values were significantly higher in the keratoconus group compared to the control group. In keratoconic patients there was a significant correlation between the axis of the shift in the LoS and the steepest keratometric axis on topography, the distance of the LoS from pupil center and vertical coma, and spherical aberration. There was also a significant correlation between the average keratometry value measured by topography and sphaerical aberration. Taking into account the changes of the LoS allows a better understanding of the pathologic optics of keratoconus, and may have a beneficial effect on increasing the precision of correcting higher order aberrations. The displacement observed in the line of sight is an internal optical compensation mechanism in order to reduce corneal aberrations.

DOI:10.14753/SE.2012.1628

7. Summary

Keratoconus is a bilateral, noninflammatory, progressive disorder characterized by corneal ectasia, thinning and protrusion. The disease induces myopia, irregular astigmatism and has well defined slit lamp findings. The diagnosis of more advanced keratoconus is not complicated, because of the typical biomicroscopic and topographic findings, but the detection of subclinical or forme fruste cases may impose difficulty. Elevation-based topography offers important advances over Placido-disc based devices. The ability to image the posterior cornea and to produce an accurate pachymetric map is itself significant. Elevation subtraction maps are also more accurate in determining the cone morphology and in separating the false-positive keratoconus suspect cases.

The aim of our study was to compare the keratometric, pachymetric and elevation parameters of normal to keratoconic corneas measured by Pentacam and to evaluate their importance in the detection of the disease. ROC curve analyses showed best predictive accuracy for posterior and anterior elevation (area under the curve: 0.97 and 0.96), followed by minimal and central pachymetry (0.89 and 0.88) in the detection of keratoconus. Optimal cutoff point for posterior elevation was found to be 15.5 μm for the discrimination of keratoconus corneas from normals. According to our results both posterior and anterior elevation, pachymetric and keratometric parameters measured by the Pentacam camera can effectively discriminate keratoconus from normal corneas serving as a useful diagnostic tool for disease staging.

The second study was designed in order to compare anterior chamber parameters in normal eyes and eyes with mild to moderate keratoconus corneas using rotating Scheimpflug imaging and evaluate trends in corneal protrusion progression. We could identify a threshold level of posterior corneal elevation (40μm) and corneal thickness (450 μm) values beyond which the level of corneal protrusion in keratoconus is accelerated.

Understanding the characteristics of ocular higher order aberrations owing to keratoconus might be very useful to differentiate early cases from simple myopia or myopic astigmatism. The purpose of our third study was to prove our hypothesis that keratoconus causes a shift in the LoS, which acts as a compensating mechanism for increased corneal higher order aberrations. To test our hypothesis, we examined location of the LoS, its position relative to the pupil center, and their impact on ocular higher order aberrations in keratoconic and control eyes. A significant shift of the line of sight was observed in keratoconic patients by aberrometry. The direction of the shift correlated with cone location and its measure correlated with vertical coma and spherical aberration.

DOI:10.14753/SE.2012.1628

8. References

1. Gefen A, Shalom R, Elad D, Mandel Y. Biomechanical analysis of the keratoconic cornea. J Mech Behav Biomed Mater. 2009;2:224-36.

2. Romero-Jiménez M, Santodomingo-Rubido J, Wolffsohn JS. Keratoconus: a review. Cont Lens Anterior Eye. 2010 ;33:157-66.

3. Rabinowitz YS. Keratoconus. Surv Ophthalmol 1998; 42:297-319. Section 3,Chapter 91.

4. Krachmer JH, Mannis MJ, Holland EJ, Palay DA. Cornea text and color atlas CD-Rom. Mosby 1998

5. Barr JT, Wilson BS, Gordon MO, et al. Estimation of the incidence and factors predictive of corneal scarring in the Collaborative Longitudinal Evaluation of Keratoconus (CLEK) Study. Cornea 2006; 25:16-25.

6. McMahon TT, Edrington TB, Szczotka-Flynn L, et al. Longitudinal changes in corneal curvature in keratoconus. Cornea 2006; 25: 296-305.

7. Swartz T, Marten L, Wang M. Measuring the cornea: the latest developments in corneal topography. Curr Opin Ophthalmol 2007; 18:325-33.

8. Konstantopoulos A, Hossain P, Anderson DF. Recent advances in ophthalmic anterior segment imaging: a new era for ophthalmic diagnosis? Br J Ophthalmol 2007; 9:1551-5.

9. Ciolino JB, Belin MW. Changes in the posterior cornea after laser in situ keratomieleusis and photorecractive keratectomy. J Cataract Refract Surg 2006; 32:1426-1431.

10. Kennedy RH, Bourne WM, Dyer JA. A 48-year clinical and epidemiologic study of keratoconus, Am J Ophthalmol 101 (1986), pp. 267–273.

11. Li X., Rabinowitz YS, Rasheed K, Yang H. Longitudinal study of the normal eyes in unilateral keratoconus patients, Ophthalmology 111 (2004), pp. 440–446.

12. Krachmer JH, Feder RS, Belin MW. Keratoconus and related noninflammatory corneal thinning disorders, Surv Ophthalmol 28 (1984), pp. 293–322.

13. Stabuc-Silih M, Strazisar M, Ravnik-Glavac M, Hawlina M, Glavac D.Genetics and clinical characteristics of keratoconus. Acta Dermatovenerol Alp Panonica Adriat. 2010;19: 3-10.

14. Barr JT, Wilson BS, Gordon MO, et al. Estimation of the incidence and factors predictive of corneal scarring in the Collaborative Longitudinal Evaluation of Keratoconus (CLEK) Study. Cornea. 2006;25:16-25.

15. Barraquer-Somers E, Chang CC, Green WR. Corneal epithelial iron deposition, Ophthalmology 1983; 90:729–734.

16. Ozdamar A, Aras C, Ustundag C, Bahcecioglu H, Ozkan S. Corneal iron ring associated with iatrogenic keratectasia after myopic laser in situ keratomileusis. J Cataract Refract Surg. 2000; 26:1684-6.

17. Suzuki H, Minarcik JR. Images in clinical medicine. Keratoconus complicated by acute corneal hydrops. N Engl J Med. 2009; 15:361-62.

18. Li X, Rabinowitz YS, Rasheed K, Yang H. Longitudinal study of the normal eyes in unilateral keratoconus patients, Ophthalmology 2004; 111: 440–446.

19. Shrapiro MB, France TD. The ocular features of Down's syndrome, Am J Ophthalmol 1985; 99:659–663.

20. Damji KF, Sohocki MM, Khan R, Gupta SK, Rahim M, Loyer M et al. Leber's congenital amaurosis with anterior keratoconus in Pakistani families is caused by the Trp278X mutation in the AIPL1 gene on 17p, Can J Ophthalmol 2001; 36:252–259.

21. Tretter T, Rabinowitz YS, Yang H et al. Aetiological factors in keratoconus, Ophthalmology 1995; 102 (Suppl):156.

22. Litcher H, Loya N, Sagie A, Cohen N, Muzmacher L, Yassur Y et al. Keratoconus and mitral valve prolapse, Am J Ophthalmol 2000; 129:667–668.

23. Määttä M, Väisänen T, Väisänen MR, Pihlajaniemi T, Tervo T. Altered expression of type XIII collagen in keratoconus and scarred human corneas: increased expression in scarred cornea is associated with myofibroblast transformation, Cornea 2006; 25:448–453.

24. Määttä M, Heljasvaara R, Sormunen R, Pihlajaniemi T, Autio-Harmainen H, Tervo T, Differential expression of collagen types XVIII/endostatin and XV in normal, keratoconus and scarred human corneas, Cornea 2006; 25: 341–349.

25. Fukuchi T, Yue BY, Sugar J, Lam S. Lysosomal enzyme activities in conjunctival tissues of patients with keratoconus, Arch Ophthalmol 1994;112: 1368–1374.

26. Sawaguchi S, Twining SS, Yue BY, Chang SH, Zhou X, Loushin G et al. Alpha 2 macroglobulin levels in normal human and keratoconus corneas, Invest Ophthalmol Vis Sci 1994; 35: 4008–4014.

27. Behndig A, Karlsson K, Johansson BO, Brännström T, Marklund SL. Superoxide dismutase isoenzymes in the human eye, Invest Ophthalmol Vis Sci 1998; 39: 471–475.

28. Kenney MC, Brown DJ. The cascade hypothesis of keratoconus, Contact Lens Anterior Eye 2003; 26: 139–146.

29. Wang Y, Rabinowitz YS, Rotter JI, Yang H Genetic epidemiological study of keratoconus: evidence for major gene determination. Am J Med Genet. 2000; 28: 403-9.

30. Rabinowitz YS, Dong L, Wistow G. Gene expression profile studies of human keratoconus cornea for NEIBank: a novel cornea-expressed gene and the absence of transcripts for aquaporin 5. Invest Ophthalmol Vis Sci. 2005; 46:1239-46.

31. Ihalainen A. Clinical and epidemiological features of keratoconus: genetic and external factors in the pathogenesis of the disease, Acta Ophthalmol 1986; 178 (Suppl): 5–64.

32. Héon E, Greenberg A, Kopp KK, Rootman D, Vincent AL, Billingsley G et al. VSX1: a gene for posterior polymorphous dystrophy and keratoconus, Hum Mol Genet 2002; 11: 1029–1036.

33. Bisceglia L, Ciaschetti M, De Bonis P, Campo PA, Pizzicoli C, Scala C et al. VSX1 mutational analysis in a series of Italian patients affected by keratoconus: detection of a novel mutation, Invest Ophthalmol Vis Sci 2005; 46: 39–45.

34. Eran P, Almogit A, David Z, Wolf HR, Hana G, Yaniv B et al. The D144E substitution in the VSX1gene: a non-pathogenic variant or disease causing mutation?, Ophthalmic Genet 2008; 29: 53–59.

35. Aldave AJ, Yellore VS, Salem AK, Yoo GL, Rayner SA, Yang H et al. No VSX1 gene mutations associated with keratoconus, Invest Ophthalmol Vis Sci 2006; 47: 2820–2822.

36. Liskova P, Ebenezer ND, Hysi PG, Gwilliam R, El-Ashry MF, Moodaley LC et al. Molecular analysis of the VSX1 gene in familial keratoconus, Mol Vis 2007; 4: 1887–1891.

37. Tang YG, Picornell Y, Su X, Li X, Yang H, Rabinowitz YS. Three VSX1 gene mutations, L159M, R166W, and H244R, are not associated with keratoconus, Cornea 2008; 27: 189–192.

38. Amsler M. Le keratocone fruste au javal, Ophthalmologica 1938; 96: 77–83.

39. Amsler M Keratocone classique et keratocone fruste, arguments unitaires. Ophthalmologica 1946; 111: 96–101.

40. McMahon TT, Anderson RJ, Roberts C, Mahmoud AM, Szczotka-Flynn LB, Raasch TW, Friedman NE, Davis LJ, CLEK Study Group. Repeatability of corneal topography measurement in keratoconus with the TMS-1. Optom Vis Sci. 2005 May;82(5):405-15

41. Rabinowitz YS, Yang H and Akkina J et al. Videokeratography of normal human corneas, Br J Ophthalmol 1996; 80: 610–616.

42. Neshburn AB, Bahri S, SalzJ. Keratoconus detected by videokeratography in candidates for photorefractive keratectomy. J Refract Surg 1995; 11: 194-201.

43. Cheng HC, Lin KK, Chen YF, Hsiao CH. Pseudokeratoconus in a patient with soft contact lens-induced keratopathy: assessment with Orbscan I. J Cataract Refract Surg. 2004; 30: 925-8.

44. Avitabile T, Franco L, Ortisi E, Castiglione F, Pulvirenti M, Torrisi B, Castiglione F, Reibaldi A. Keratoconus staging: a computer-assisted ultrabiomicroscopic method compared with videokeratographic analysis. Cornea. 2004 Oct;23(7):655-60.

45. Smolek MK, Klyce SD. Current keratoconus detection methods compared with a neural network approach. Invest Ophthalmol Vis Sci. 1997; 38:2290-9.

46. Rabinowitz YS, Yang H, Elashoff J, Rotter J. The KI-SA% index: a quantitative new videokeratography algorithm embodying minimal topographic criteria for diagnosing keratoconus and "suspects" (abstract), Invest Ophthalmol Vis Sci 1996; 37: S910.

47. Rabinowitz YS. Videokeratographic indices to aid in screening for keratoconus. J Refract Surg 1995; 11:371-379.

48. Fam HB, Lim KL. Corneal elevation indices in normal and keratoconic eyes. J Cataract Refract Surg 2006;32:1281-1287.

49. Ambrósio R, Alonso RS, Luz A, Velarde LGC. Corneal-thickness spatial profile and corneal-volume distribution: Tomographic indices to detect keratoconus. J Cataract Refract Surg 2006; 32:1851-1859.

50. Tomidokoro A, Oshika T, Amano et al. Changes in anterior and posterior corneal curvatures in keratoconus. Ophthalmology 2000; 107:1328-1332.

51. Wilson SE. Cautions regarding measurement of the posterior corneal curvature. Ophthalmology 2000; 107:1223.

52. De Sanctis U, Missolunghi A, Mutani B, et al. Reproducibility and repeatability of central corneal thickness measurement in keratoconus using the rotating Scheimpflug camera and pachymetry. Am J Ophthalmol 2007; 144: 712-718.

53. Emre S, Doganay S, Yologlu S. Evaluation of anterior segment parameters in keratoconic eyes measured with the Pentacam system. J Cataract Refract Surg 2007; 33:1708-1712.

54. Kawana K, Miyata K, Tokunaga T, et al. Central corneal thickness measurements using Orbscan II scanning slit topography, noncontact specular microscopy, and ultrasonic pachymetry in eyes with keratoconus. Cornea; 2005;24:967-71.

55. Ho T, Cheng ACK, Rao SK, et al. Central corneal thickness measurements using Orbscan II, Visante, ultrasound, and Pentacam pachymetry after laser in situ keratomileusis for myopia. J Cataract Refract Surg 2007; 33:1177-1182.

56. Chen D, Lam AKC. Intrasession and intersession repeatability of the Pentacam system on posterior corneal assessment in the normal human eye. J Cataract Refract Surg 2007; 33:448-454.

57. Ucakhan OO, Ozkan M, Kanpolat A. Corneal thickness measurements in normal and keratoconic eyes: Pentacam comprehensive eye scanner versus noncontact specular microscopy and ultrasound pachymetry. J Cataract Refract Surg 2006; 32:970-977.

58. Nilforoushan MR, Marmor M, Abramson J, et al. Comparative evaluation of refractive surgery candidates with Placido topography, Orbscan II, Pentacam, and wavefront analysis. J Cataract Refract Surg 2008; 34: 623-631

59. Quisling S, Sjoberg S, Zimmerman B, Goins K. Comparison of Pentacam and Orbscan II on posterior curvature topography measurements in keratoconus eyes. Ophthalmology 2006; 113:1629-1632

60. Rüfer S, Schröder A, Arvani MK, et al. Central and peripheral corneal pachymetry – standard evaluation with the Pentacam system. Klin Monatsbl Augenheilkd 2005; 222:117-122.

61. Kosaki R, Maeda N, Bessho K, et al. Magnitude and orientation of Zernike terms in patients with keratoconus. Invest Ophthalmol Vis Sci 2007;48:3062-8.

62. Oie Y, Maeda N, Kosaki R, et al. Characteristics of ocular higher-order aberrations in patients with pellucid marginal corneal degeneration. J Cataract Refract Surg 2008;34:1928-34.

63. Nakagawa T, Maeda N, Kosaki R, et al. Higher-order aberrations due to the posterior corneal surface in patients with keratoconus.Invest Ophthalmol Vis Sci 2008 Nov "in press".

64. Pantanelli S, MacRae S, Jeong TM, Yoon G. Characterizing the wave aberration in eyes with keratoconus or penetrating keratoplasty using a high-dynamic range wavefront sensor. Ophthalmology 2007;114:2013-21.

65. Bühren J, Kühne C, Kohnen T. Defining subclinical keratoconus using corneal first-surface higher-order aberrations. Am J Ophthalmol 2007;143:381-9.

66. Shah S, Naroo S, Hosking S, et al. Nidek OPD-scan analysis of normal, keratoconic, and penetrating keratoplasty eyes. J Refract Surg 2003;19:S255-9.

67. Maeda N. Clinical applications of wavefront aberrometry - a review. Clin Experiment Ophthalmol. 2009;37: 118-29.

68. Kirwan C, O'Malley D, O'Keefe M. Corneal hysteresis and corneal resistance factor in keratoectasia: findings using the Reichert ocular response analyzer, Ophthalmologica 2008; 222: 334–337.

69 Kirwan C, O'Keefe M. Corneal hysteresis using the Reichert ocular response analyser: findings pre- and post-LASIK and LASEK, Acta Ophthalmol 2008; 86: 215–218.

70. Kida T, Liu JH, Weinreb RN. Effects of aging on corneal biomechanical properties and their impact on 24-hour measurement of intraocular pressure, Am J Ophthalmol 2008; 146: 567–572.

71. Lim N, Vogt U. Characteristics and functional outcomes of 130 patients with keratoconus attending a specialist contact lens clinic, Eye 2002; 16: 54–59.

72. Marsack JD, Parker KE, Applegate RA. Performance of wavefront-guided soft lenses in three keratoconus subjects, Optom Vis Sci 2008; 85: E1172–78.

73. Zadnik K, Barr JT, Steger-May K, Edrington TB, McMahon TT, Gordon M. Comparison of flat and steep rigid contact lens fitting methods in keratoconus, Optom Vis Sci 2005;82: 1014–1021.

74. Wollensak G. Crosslinking treatment of progressive keratoconus: new hope. Curr Opin Ophthalmol. 2006; 17:356-60.

75. Koller T, Seiler T. Therapeutic cross-linking of the cornea using riboflavin/UVA. Klin Monbl Augenheilkd. 2007; 224: 700-6.

76. Koller T, Mrochen M, Seiler T.Complication and failure rates after corneal crosslinking. J Cataract Refract Surg. 2009; 35:1358-62.

77. Alió JL, Piñero DP, Söğütlü E, Kubaloglu A. Implantation of new intracorneal ring segments after segment explantation for unsuccessful outcomes in eyes with keratoconus. J Cataract Refract Surg. 2010 ;36: 1303-10.

78. Rabinowitz YS.INTACS for Keratoconus.Int Ophthalmol Clin. 2010; 50:63-76.

79. Alió JL, Shabayek MH, Artola A.Intracorneal ring segments for keratoconus correction: long-term follow-up. J Cataract Refract Surg. 2006;32: 978-85.

80. Tan BU, Purcell TL, Torres LF, Schanzlin DJ. New surgical approaches to the management of keratoconus and post-LASIK ectasia. Trans Am Ophthalmol Soc. 2006;104: 212-20.

81. Tan DT, Por YM. Current treatment options for corneal ectasia. Curr Opin Ophthalmol. 2007; 18:284-9.

82. Pramanik S, Musch DC, Sutphin JE, et al. Extended long-term outcomes of penetrating keratoplasty for keratoconus. Ophthalmology 2006; 113:1633–1638.

83. Zadok D, Schwarts S, Marcovich A, et al. Penetrating keratoplasty for keratoconus. Long term results. Cornea 2005; 24:959–961.

84. Al-Torbak AA, Al-Motowa S, Al-Assiri A, et al. Deep anterior lamellar keratoplasty for keratoconus. Cornea 2006; 25:408–412.

85. Tan DT, Ang LPK. Automated lamellar therapeutic keratoplasty for post-PRK corneal scarring and thinning. Am J Ophthalmol 2004; 138:1067–1069.

86. Tzelikis PF, Cohen EJ, Rapuano CJ, et al. Management of pellucid marginal degeneration. Cornea 2005; 24:555–560.

87. Cheng CL, Theng JT, Tan DT. Compressive C-shaped lamellar keratoplasty: a surgical alternative for the management of severe astigmatism from peripheral corneal degeneration. Ophthalmology 2005; 112:425–430.

88. Módis L, Sohajda Z, Komár T, Hassan Z, Berta A. Clinicopathological characteristic of keratoglobus. Klin Monbl Augenheilkd. 2005; 222:505-8.

89. Randleman JB. Post-laser in-situ keratomileusis ectasia: current understanding and future directions. Curr Opin Ophthalmol. 2006; 17:406-12.

90. Dupps WJ Jr. Biomechanical modeling of corneal ectasia. J Refract Surg 2005; 21:186–190.

91. Binder PS. Ectasia after laser in situ keratomileusis. J Cataract Refract Surg. 2003; 29: 2419-29.

92. Binder PS, Lindstrom RL, Stulting RD, et al. Keratoconus and corneal ectasia after LASIK. J Cataract Refract Surg 2005; 31:2035–2038.

93. Németh J, Erdélyi B, Csákány B.Corneal topography changes after a 15 second pause in blinking. J Cataract Refract Surg. 2001; 27:589-92.

94. Applegate RA, Thibos LN, Twa MD, Sarver EJ. Importance of fixation, pupil center, and reference axis in ocular wavefront sensing, videokeratography, and retinal image quality. J Cataract Refract Surg. 2009; 35:139-52.

95. Reinstein DZ, Archer TJ, Couch D. Accuracy of the WASCA aberrometer refraction compared to manifest refraction in myopia. J Refract Surg 2006;22:268-74.

96. Cervino A, Hosking SL, Rai GK et al. Wavefront analyzers induce instrument myopia. J Refract Surg 2006;22:795-803.

97. Thibos LN, Applegate RRA, Schwiegerling JT, Webb R. Visison science and its applications: standards for reporting the optical aberrations of eyes. J Refract Surg 2002;18:S652-60.

98. Applegate RA, Thibos LN, Bradely A, et al. Reference axis selection: subcommittee report of the OSA working group to establish standards for measurement and reporting of optical aberrations of the eye. J Refract Surg 2000;16:S656-8.

99. Smolek MK, Klyce SD, Sarver EJ. Inattention to nonsuperimposable midline symmetry causes wavefront analysis error. Arch Ophthalmol 2002;120: 439-47.

100. Alpins NA. Astigmatism analysis by the Alpins method. J Cataract Refract Surg 2001; 27:31-49.

101. Eydelman MB, Drum B, Holladay J et al. Standardized analysis of correction of astigmatism by laser systems that reshape the cornea. J Refract Surg 2006; 22: 81-95.

102. Hanley JA, Negassa A, Edwardes MD, Forrester JE. Statistical analysis of correlated data using generalized estimating equations: an orientation, Am J Epidemiol 2003; 157: 364–375.

103. Martus P, Jünemann A, Wisse M. Multivariate approach for quantification of morphologic and functional damage in glaucoma. Invest Ophthalmol Vis Sci 2000; 41:1099-1110

104. De Sanctis U, Loiacono C, Richiardi L, et al. Sensitivity and Specificity of Posterior Corneal Elevation Measured by Pentacam in Discriminating Keratoconus/Subclinical Keratoconus. Ophthalmology 2008; 115:1534-1539.

105. Cairns G, McGhee CN. Orbscan computerized topography: attributes, applications, and limitations. J Cataract Refract Surg 2005; 31:205-220.

106. Rao SN, Raviv T, Majmudar PA, Epstein RJ. Role of Orbscan II in screening keratoconus suspects before refractive corneal surgery. Ophthalmology 2002; 109:1642-1646.

107. Meinhardt B, Stachs O, Stave J, Beck R, Guthoff R. Evaluation of biometric methods for measuring the anterior chamber depth in the non-contact mode, Graefes Arch Clin Exp Ophthalmol 2006;244: 559–564.

108. Buehl W, Stojanac D, Sacu S, Drexler W, Findl O. Comparison of three methods of measuring corneal thickness and anterior chamber depth, Am J Ophthalmol 2006; 141: 7–12.

109. Mollan SP, Wolffsohn JS, Nessim M, Laiquzzaman M, Sivakumar S, Hartley S, Shah S. Accuracy of Goldmann, ocular response analyser, Pascal and TonoPen XL tonometry in keratoconic and normal eyes, Br J Ophthalmol 2008; 92:1661–1665.

110. Wollensak G, Spoerl E, Seiler T. Riboflavin/ultraviolet-A-induced collagen crosslinking for the treatment of keratoconus, Am J Ophthalmol 2003; 135: 620–627.

111. Alio JL, Shabayek MH. Corneal higher order aberrations: a method to grade keratoconus. J Refract Surg 2006;22:539-45.

112. Jafri B, Li X, Yang H, Rabinowitz YS. Higher order wavefront aberrations and topography in early and suspected keratoconus. J Refract Surg 2007; 23:774-81.

113. Lim L, Wei RH, Chan WK, Tan DTH. Evaluation of higher order ocular aberrations in patients with keratoconus. J Refract Surg 2007; 23:825-8.

114. Maeda N, Fujikado T, Kuroda T et al. Wavefront aberrations measured with Hartmann-Shack sensor in patients with keratoconus. Ophthalmology 2002;109: 1996-2003.

115. Negishi K, Kumanomido T, Utsumi Y, Tsubota K. Effect of higher-order aberrations on visual function in keratoconic eyes with a rigid gas permeable contact lens. Am J Ophthalmol 2007;144: 924-9.

116. Klein SA, Garcia DD. Line of sight and alternative representations of aberrations of the eye. J Refract Surg 2000;11:S630-5.

117. Bueeler M, Iseli HP, Jankov M, Mrochen M. Treatment-induced shifts of ocular reference axes used for measurement centration. J Cataract Refract Surg 2005; 31:1986-94.

118. Calossi A. Corneal asphericity and spherical aberration. J Refract Surg 2007;23:505-14.

119. Salmon TO, Thibos LN. Videokeratoscope-line-of sight misalignement and its effect on measurements of corneal and internal ocular aberrations. J Opt Soc Am A Opt Image Sci Vis 2002;19:657-69.

120. Kollbaum PS, Bradley A. Correcting aberrations with contact lenses. Contact Lens Spectrum 2007 November, 24-31.

121. Kelly J, Mihashi T, Howland. Compensation of corneal horizontal/vertical astigmatism, lateral coma, and spherical aberration by internal optics of the eye. Journal of Vision 2004; 4:262-71.

122. Artal P, Benito A, Tabernero J. The human eye is an axample of robust optical design. Journal of Vision 2006; 6:1-7.

123. Zhang X, Ye M, Bradley A, Thibos L. Apodization by the Stiles-Crawford effect moderates the visual impact of retinal image defocus. Opt Soc Am A Opt Image Sci Vis 1999; 16:812-20.

124. Westheimer G. Directional sensitivity of the retina: 75 years of Stiles-Crawford effect. Proc Biol Sci. 2008; 275:2777-86.

125. Tan B, Baker K, Chen YL et al. How keratoconus influences optical performance of the eye. Journal of Vision 2008; 13:1-10.

DOI:10.14753/SE.2012.1628

9.List of publications

Publications attached to Ph.D. thesis

I. Miháltz K, Kovács I, Takács A, Nagy ZZ. Evaluation of keratometric, pachymetric and elevation parameters of keratoconic corneas with Pentacam. Cornea. 2009; 28:976-80. **IF:2.106**

II. Miháltz K, Kránitz K, Kovács I, Takács Á, Németh J, Nagy ZZ: Shifting of the line of sight in keratoconus measured by a Hartmann-Shack sensor. Ophthalmology.2010;117:41-48. **IF:5.491**

III. Kovács I, Miháltz K, Németh J, Nagy ZZ. Anterior chamber characteristics of keratoconus measured by rotating Scheimpflug camera. J Cat Refr Surg. 2010; 36: 1101-1106. **IF:2.745**

IF: 10,342

Publications not attached to Ph.D. thesis

Publications in Hungarian journals:

1. Miháltz K, Vámos R, Salacz Gy. A cornea endotheliumának spekulár mikroszkópos vizsgálata kontaktlencsét viselőkön. Szemészet. 2002.139, 183-186.

2. Miháltz K, Salacz Gy. A száraz szem és kezelése. Hyppocrates. 2003.V.41-44.

3. Miháltz K, Récsán Zs, Radó G, Salacz Gy. Corneaperforációhoz vezető autoimmun kórképek. Szemészet. 2004.141,83-88.

4. Nagy Z Z, Miháltz K, Filkorn T, Takács Á, Németh J. A corneális crosslinking szerepe a keratoconus kezelésében – előzetes eredmények. Szemészet. 2008. 145, 85-88.

DOI:10.14753/SE.2012.1628

5. Kránitz K, Miháltz K, Kovávs I, Takács A, Nagy Z Z. A hummámfront-aberrációk szerepe a keratoconus diagnosztikájában
2010. 147; 28-32.

Publications in foreign journals:

1. Somfai GM, Miháltz K, Tulassay E, Rigó J Jr. Diagnosis of serous neuroretinal detachments of the macula in severe preeclamptic patients with optical coherence tomography. Hypertens Pregnancy. 2006;25(1):11-20.

2. Miháltz K, Takács A, Filkorn T, Nagy ZZ: Outcome of iris and lens perforation during keratoplasty for keratoconus. South-East European Journal of Ophthalmology 2008; 2(3-4): 51-54.

3. Takács A, Miháltz K, Nagy ZZ. Evaluation of corneal density and haze with the rotating Scheimpflug camera after photorefractive keratectomy in myopic and hyperopic patients. J Refract Surg. 2010 Jul 13:1-9. doi: 10.3928/1081597X-20100618-02

Papers accepted for publication:

1. Kovács I, Miháltz K, Ecsedy M, Németh J, Nagy ZZ. The role of reference body selection in calculating posterior corneal elevation and prediction of keratoconus using rotating Scheimpflug camera. Acta Ophthalmologica. (accepted for publication) doi: 10.1111/j.1755-3768.2010.02053.x

2. Miháltz K, Kovács I, Kránitz K, Erdei G, Németh J, Nagy ZZ. The mechanism of aberration balance and its effect on retinal image quality in keratoconus. J Cat Refr Surg. (accepted for publication)

Cumulative: IF: 17,658

Presentations, posters, abstracts in the topic of the Ph.d. thesis:

DOI:10.14753/SE.2012.1628

International:

1. Miháltz K, Kránitz K, Kovács I, Nagy ZZ. Evaluation of Wavefront Aberrations in Patients With Keratoconus Measured With a Hartmann-Shack Sensor. Invest Ophthalmol Vis Sci. 2009: ARVO E-Abstract 3541

2. Kovács I, Miháltz K, Takács A, Kránitz K, Nagy ZZ. Evaluation of the Effect of Corneal Protrusion on Anterior Chamber Morphology in Keratoconic Patients Using Pentacam Scheimpflug Camera. Invest Ophthalmol Vis Sci. 2009: ARVO E-Abstract 3531

3. Miháltz K, Kovács I, Takács A, Nagy ZZ. Assessment of elevation parameters in keratoconus. Congress of the European Society of Cataract and Refractive Surgery (ESCRS), Barcelona, Spain, 2009 September, poster

4. Miháltz K, Kovács I, Kránitz K, Németh J, Nagy ZZ. Wavefront aberrometry characteristics and their effect on visual metrics measured by a Hartmann-Schack sensor in keratoconus. Congress of the European Society of Cataract and Refractive Surgery (ESCRS), Budapest, 2010 February, free paper

5. Kovács I, Miháltz K, Ecsedy M, Kránitz K, Németh J, Nagy ZZ. The role of reference body selection in calculating posterior corneal elevation and prediction of keratoconus using rotating Scheimpflug camera. Congress of the European Society of Cataract and Refractive Surgery (ESCRS), Budapest, 2010 February, free paper

6. Miháltz K, Kovács I, Kránitz K, Erdei G, Nagy ZZ. The mechanism of aberration balance and its effect on retinal image quality in keratoconus. Congress of the European Society of Cataract and Refractive Surgery (ESCRS), Paris, 2010 September, poster

Hungarian:

1. Miháltz K, Nagy ZZ. Topographic characteristics of keratoconus patients. Congress of the Hungarian Ophthalmologic Society, Pécs, 2008 May, free paper

DOI:10.14753/SE.2012.1628

2. Miháltz K, Nagy ZZ. Topographic and aberrometric characteristics of keratoconus. Continuation course of the Department of Ophthalmology, Semmelweis University. 2008 December, course

3. Miháltz K, Nagy ZZ. Aberrometric characteristics of keratoconus. Congress of the Hungarian Ophthalmologic Society. Budapest, 2009 June, course

4. Miháltz K, Nagy ZZ . Aberrometric characteristics of keratoconus. Continuation course of the Department of Ophthalmology, Semmelweis University. 2010 January, course

5. Miháltz K, Nagy ZZ. Wavefront analyses of keratoconic patients. Congress of the Hungarian Ophthalmologic Society, Szeged, 2010 June, course

Presentations, posters, abstracts not in the topic of the Ph.d. thesis:

International:

1. Miháltz K, Radó G, Salacz Gy. Corneal amnion covering. Congress of the Romanian Society of Ophthalmology, Timisoara, 2002 April, free paper

2. Radó G, Miháltz K, Salacz Gy. Corneal amnion covering in patients suffering from Mooren ulcer. Congress of the German Society of Ophthalmology (DOG), 2001 September, Berlin, free paper

3. Radó G, Miháltz K, Salacz Gy. Carbon dioxide laser treatment in partial limbal deficiency. Congress of the German Society of Ophthalmology (DOG), Berlin, 2002 September, free paper

4. Radó G, Miháltz K, Salacz Gy. Fixation of the Iris-claw Lens. of the German Cataract Surgeons, Ludwigshafen, 2003 February, free paper

DOI:10.14753/SE.2012.1628

5. Miháltz K, Győry J, Salacz Gy: Angiographic evidence of choroidal thrombosis in toxaemia of pregnancy – A case report. 14th Congress of Societas Ophthalmologica Europaea (SOE), Madrid, 2003 June, poster

6. Kovács I, Rigo J, Miháltz K, Somfai GM. Serous neuroretinal detachment of the macula diagnosed by optical coherence tomography in patients with severe preeclampsia. 9th Vision Research Conference – Neuroimaging the Retina. Fort Lauderdale 2005, Poster Nr: 16

7. Nagy ZZ, Takács A, Kránitz K, Miháltz K. Comparative analysis of femtolaser-assisted and manual capsulorhexis during phacoemulsification. Congress of the European Society of Cataract and Refractive Surgery (ESCRS), Paris, 2010 September, free paper

Hungarian:

1. Miháltz K, Radó G. Amnion covering of eyes with ulcus Mooren. Congress of the Hungarian Ophthalmologic Society Miskolc, 2002 August, free paper

2. Miháltz K. Autoimmun diseases leading to cornea perforation. Congress of the Hungarian Ophthalmologic Society. Budapest, 2003 August, free paper

3. Miháltz K, Takács Á, Somfai G, Nagy ZZ. Topographic and refractive characteristics of myopic patients. Societas Hungarica ad Implantandam Oculi Lenticulam (SHIOL), Keszthely, 2008 March, free paper

4. Miháltz K, Nagy ZZ . Anterior segment characteristics of different refractive states of the eye. Societas Hungarica ad Implantandam Oculi Lenticulam (SHIOL), Keszthely, 2009 March, free paper

DOI:10.14753/SE.2012.1628

Acknowledgement

First and foremost, I would like to thank to my supervisor, Dr. Zoltán Nagy for the valuable guidance and advice. He inspired me to work in this scientific project. I also would like to thank him for providing instrumental facilities to complete my researches.

Besides, I would like to thank the head of our Department, Dr. János Németh for supporting my research and for providing a good environment to this work. Also, I would like to take this opportunity to thank Dr. Kinga Kránitz, Dr. Ágnes Takács and Judit Zadravecz for the great help in data acquisition. In addition, I would also like to thank to Dr. Illés Kovács, who provided me valuable help in statistics and for his guidance in writing my articles.

Finally, an honorable mention goes to my family and friends for their understandings and supports in completing this work.